



**Cornell University  
Environmental  
Health and Safety**

**Cheryl Brown**

Environmental Project  
Manager

Suite 210, 395 Pine Tree Road

Ithaca, New York 14850

t. 607.254.8687

f. 607.255.8267

e. [cah65@cornell.edu](mailto:cah65@cornell.edu)

[www.ehs.cornell.edu](http://www.ehs.cornell.edu)

April 25, 2016

NYSDEC Regional Water Engineer  
NYSDEC Region 7  
615 Erie Boulevard West  
Syracuse, NY 13204-2400

Re: Third 24-Month Status Report - Lake Source Cooling Outfall Redesign  
Cornell University Lake Source Cooling SPDES Permit # NY 0244741

Dear Regional Water Engineer:

This transmittal satisfies the third Status Report deliverable in the Schedule of Submittals for Outfall Redesign Requirements in the Lake Source Cooling (LSC) SPDES Permit # NY 0244741, which requires the submittal of a status report every 8 months after the effective date of approval (EDA) of the Outfall Redesign Study. The EDA is May 1, 2014, and the first and second status reports were submitted to the NYSDEC on Dec. 22, 2014 and Aug. 24, 2015, respectively, with the third status report due by May 1, 2016.

The enclosed third Outfall Redesign Status Report is being submitted in accordance with SPDES requirements. Please contact me should you have any questions related to this submittal.

Sincerely,

Cheryl A. Brown  
Environmental Project Manager

Enclosure

xc: Bureau of Water Permits, NYSDEC Albany  
Jeff Myers, NYSDEC  
Steve Beyers, Cornell University  
Edwin (Todd) Cowen, Cornell University  
W. S. (Lanny) Joyce, Cornell University  
Liz Moran, Ecologic

# Status Report 3

## Lake Source Cooling

# Outfall Redesign Study

SPDES Number NY0244741

4/25/2016

Department of Energy & Sustainability

Cornell University

Infrastructure, Properties & Planning

## Table of Contents

---

1. Introduction.....	2
2. Summary of Progress by Workplan Task.....	4
3. Status of the Three-Dimensional Hydrodynamic Model Si3D.....	6
3.1 Previously Reported .....	6
3.2 Current Focus .....	7
4. Problems Encountered and Impact on Schedule .....	8
5. Upcoming Tasks.....	8
6. Attachment: Technical Report.....	9

## 1. Introduction

---

Cornell University's Lake Source Cooling (LSC) facility supplies chilled water to air condition and dehumidify buildings on the university's Ithaca campus, and cool research equipment and spaces. The LSC process uses the renewable resource, naturally cold water deep in Cayuga Lake, in a non-polluting heat exchange process. This process draws water from deep in Cayuga Lake, where temperatures remain cold year-round, and circulates lake water through a heat exchange facility, located on East Shore Drive in Ithaca. The lake water transfers its chill to a second closed loop of water that is connected to the campus cooling system. Slightly warmed water is returned to southern Cayuga Lake through an underwater diffuser. The lake water and campus chilled waters never mix.

The New York State Department of Environmental Conservation (NYSDEC) issued a State Pollutant Discharge Elimination System (SPDES) permit for the LSC facility in March 1998, once all the environmental reviews were completed. The permit, regulating the return of the slightly-warmed lake water to Cayuga Lake, has been renewed periodically since the LSC facility came on line in July, 2000. The most recent SPDES permit, effective date May 1, 2013, included several modifications and new conditions. This status report #3 summarizes work accomplished to date on one of the May 1, 2013 permit requirements: to complete a preliminary redesign study for a modified outfall of the LSC facility. A modification to the outfall would be implemented in the event that Cornell determines that this action would be the most practical and cost-effective approach to comply with a future phosphorus limit, or to avoid the risk of adverse environmental impacts to Cayuga Lake.

The language from the SPDES permit requiring the LSC outfall redesign study is cited below.

"In compliance with Title 8 of Article 17 of the Environmental Conservation Law of New York State and in compliance with the Clean Water Act, as amended, (33 U.S.C. 1251 et. Seq.), per SPDES Permit Number NY 0244741 ([http://www.dec.ny.gov/docs/water\\_pdf/cornellscprmt.pdf](http://www.dec.ny.gov/docs/water_pdf/cornellscprmt.pdf)), effective May 1, 2013, Cornell (permittee) shall comply with the following schedule for permit compliance:

"The permittee shall develop and submit an approvable plan for an Outfall Redesign Study to evaluate potential alternative sites for relocating the discharge from Outfall 001 to a location within the Class AA segment of Cayuga Lake (as depicted by transect A-A' on the Monitoring Locations map and defined in 6 NYCRR Part 898.4, Table I, Item 227).

"The requirement of this Study shall be to evaluate the current mixing zone of the discharge, identify one or more discharge locations in waters of sufficient depth to ensure that the discharge plume remains below the photic zone and to determine that the discharge will not contribute to an impairment of the designated uses of the Lake."

Cornell University developed a draft workplan for completion of the required outfall redesign study, and met with NYSDEC staff in Albany NY in December 2013 to discuss the technical elements of our approach. The draft workplan was modified in response to discussion during the December meeting; a

final version of the workplan was submitted to NYSDEC in January 2014. The workplan was approved, with one additional requirement, on May 1, 2014. This date (effective date of workplan approval, EDA) defines the schedule set forth in the May 1, 2013 SPDES permit for the required status reports and final report of the outfall redesign study.

The permittee shall submit Outfall Redesign Study status reports: EDA + 8 months (Jan 1, 2015)  
EDA + 16 months (Sept. 1, 2015)  
EDA + 24 months (May 1, 2016)

The permittee shall submit an approvable final report: EDA + 30 months (Nov. 1, 2016)

**This document is Status Report 3, submitted EDA+24 months, on or before May 1, 2016.**

## 2. Summary of Progress by Workplan Task

The approved workplan includes a table of objectives and tasks that will enable Cornell to meet the outfall redesign-related requirements of the May 1, 2013 SPDES permit for the LSC facility. The objectives and tasks are summarized in [Table 2-1](#) along with a brief status update as of EDA + 24 months. One additional task requested by NYSDEC as part of the workplan approval is designated in blue text.

**Table 2-1. Summary of progress with workplan tasks**

Objective	Task	Status Update EDA+ 24 months
<p><b>Evaluate current mixing zone of the LSC return flow</b></p>	<p>Complete a three-dimensional (3D) model of the LSC return flow under current conditions: flow rate and temperature of LSC return flow; meteorological forcing functions; diffuser configuration; flow rates from IAWWTP and VCHWWTP.</p> <hr/> <p>Validate the 3D model using data from the RUSS, thermistor at the pile cluster, LSC intake temperature records, and other measurements specifically for this study.</p> <hr/> <p>Use the validated model to simulate the 3D velocity and temperature fields under current conditions, from which estimates of the spatio-temporal evolution of the LSC outfall plume will be determined.</p> <hr/> <p>Quantify the effects of the LSC return flow on residence time of Cayuga Lake water on the shelf.</p>	<p><b>Underway</b></p> <p>Alexandra King and Edwin Cowen continue to make substantial progress with setting up and testing the three-dimensional hydrodynamic model of the southern shelf of Cayuga Lake, Si3D. A detailed report of their progress with model calibration and validation is included as an <b>Attachment</b>.</p> <p>As reported in <b>Status Report 1</b>, current conditions of mixing and water residence time on the shelf have been analyzed under various conditions of stream flow and wind conditions. The existing LSC outfall diffuser was analyzed using CORMIX to characterize the near-field mixing dynamics; this enabled the researchers to modify the governing equations within Si3D to accommodate near-field mixing.</p> <p>In <b>Status Report 2</b>, we described how data from a detailed gridding study completed in August 2014 were being used to calibrate the near-field model. This calibration will continue into May 2016.</p>

<b>Identify an alternative discharge location that meets criteria</b>	Define the depth of photic zone in Cayuga Lake, based on statistical analysis of light profile data in Class AA segment collected 1999-2006, 2013.	<b>Complete</b> , reported in Status Report 1.
	Apply model to a new outfall located within the Class AA segment of Cayuga Lake in order to project the configuration of the discharge plume of LSC return flow during the critical period for phytoplankton growth (June 1-Sept 30).	<b>Complete</b> , reported in Status Report 1.
	<b>Discuss the potential impact of return LSC flow through a new outfall during May and October (per NYSDEC request 5/1/14)</b>	<b>Complete</b> , reported in Status Report 1.
	Investigate potential effects of a range of meteorological conditions on projected plume from a relocated outfall.	<b>Complete</b> , reported in Status Report 1.
<b>Compare environmental impacts of existing and alternative outfall</b>	Apply the hydrodynamic and eutrophication models to project summer phosphorus and chlorophyll concentrations in 303(d) listed (Class A, southern shelf) segment and main lake (Class AA segment) of Cayuga Lake, under two scenarios: current outfall and redesigned outfall.	<b>Pending</b> (scheduled with completion of the eutrophication model in third quarter 2016)
<b>Develop alternative outfall</b>	Complete conceptual design of outfall extension/relocation	<b>Underway</b> (30% complete) Conceptual design solutions have been explored and will be further developed as necessary when modeling is complete
	Develop (engineers opinion of) costs for permitting, design, survey, bidding, construction	<b>Underway</b> (30% complete)
<b>Prepare detailed implementation schedule</b>	Identify potential suppliers and contractors; develop critical path timeline for acquisition of pipe and other materials.	<b>Underway</b> (30% complete)
	Identify required regulatory permits and approvals from NYSDEC, ACOE, and any local municipalities; including SEQRA compliance	<b>Underway</b> (30% complete)
	Identify required easements from OGS	<b>Underway</b> (30% complete)
<b>Submit outfall redesign study to NYSDEC</b>	Report to comply with SPDES special condition	<b>Pending</b> Scheduled EDA+30 months, 11/1/2016

### 3. Status of the Three-Dimensional Hydrodynamic Model Si3D

---

#### 3.1 Previously Reported

---

##### **January 2015 Status Report #1 (SR1) included discussion of**

1. Development of the numerical grid/mesh for the 3D model (refer to SR1, Section 3.1).
2. Field data collected in 2012, 2013, and 2014 (refer to SR1, Section 3.2).
3. Analysis of the LSC outfall operating parameters and ambient lake conditions. Includes classification of the outfall according to the CORMIX II classification system (refer to SR1, Section 3.3).
4. Modifications to the 3D hydrodynamic model, Si3D, in order to:
  - a) incorporate the LSC outfall's input of mass, momentum, and buoyancy (and the intake's sink for these quantities) into the model equations, and
  - b) modify horizontal eddy viscosity and diffusivity in the near field of the outfall plume to ensure linear spreading with an adjustable entrainment rate (SR1, Section 3.4)

##### **September 2015 Status Report #2 (SR2) included discussion of continued progress with calibrating the near-field plume dynamics for incorporation into the shelf-wide Si3D model.**

1. The Cornell research team conducted an intensive temperature monitoring field study (gridding study) in August 2014 to map the LSC outfall plume. Temperature profiles were measured at 170 points centered near the LSC outfall, and three continuous temperature records were collected at the edges of the sampling domain using thermistor strings.
  - a) The gridding study results are being used to calibrate the single parameter that can be calibrated (designated *alpha*); this sets the near-field entrainment rate.
  - b) Dr. Alexandra King and Professor Edwin Cowen reported substantial progress in compiling the input files needed to run the model simulations.

## 3.2 Current Focus

---

The Cornell research team has prepared a detailed report of their progress with calibration and validation of the Si3D model of the Cayuga Lake shelf region, incorporating the LSC return flow diffuser. Their technical report is included as an **Attachment**. An executive summary is included in this section of SR-3.

### ***Executive Summary***

The April 2016 Technical Report by Dr. Alexandra King and Professor Edwin Cowen provides a detailed explanation of their progress with incorporating the return flow from the LSC outfall diffuser into the model Si3D. The researchers' initial approach, described in the 2015 SR1, was not successful (i.e., the mathematical solution to the model equations did not converge for an idealized test case). They derived an analytical solution to describe horizontal diffusivity of the LSC plume behavior in the near-field and intermediate field, and programmed this explicit solution into the Si3D code. Section 1 of the Technical Report outlines the improvements to the diffuser submodel and explains how it is incorporated into Si3D. The revised model will be calibrated using the 2014 gridding data set.

Although the diffuser model is not yet calibrated, the researchers have set up season-long simulations for 2012, 2013, and 2014. These simulations will be re-executed once the final version of the code is ready. Section 2 of the Technical Report describes the bathymetric grid, model drivers, and the data that will be used to test model performance. In addition, performance of the non-calibrated code is examined using the root mean square error (RMSE) metric to compare model predictions with measured temperatures and velocities. In Section 3, the effects of initial conditions are explored, along with preliminary sensitivity analyses for model parameters.

Once the calibration is complete, the Si3D model will be validated by comparison to other data sets. The validated model will then be used in a predictive manner, to simulate the velocity and water temperature conditions under current conditions and alternative scenarios of the LSC outfall location and configuration. The impacts of the LSC return flow on residence time of water on the shelf will then be assessed.

#### 4. Problems Encountered and Impact on Schedule

---

The outfall redesign study remains on track for completion within the permit-required 30 month period. There is one schedule-related qualification; the deadline to complete the water quality model is two months after the deadline to submit an approvable outfall redesign study. We have conferred with the UFI water quality modeling team and anticipate that the model projections relevant to the outfall redesign study will be done in time to meet our November 1, 2016 deadline. However, these model runs may be characterized as preliminary if technical reviews of the model are not completed by the submittal date for the final outfall redesign study.

#### 5. Upcoming Tasks

---

- Complete the calibration and validation of Si3D model, then proceed with using the model in a predictive manner to estimate water residence time on the shelf with LSC outfall in place or at the alternative location within the Class AA segment.
- Once the eutrophication model is calibrated and validated, complete projections of the concentration of Particulate Organic Carbon (surrogate for phytoplankton biomass) under two scenarios: current and alternate LSC outfall locations. We note that these two model runs may be characterized as “Preliminary, pending completion of external reviews of the Cayuga Lake Water Quality Model”. This qualification may be needed due to the difference in completion dates for the outfall redesign study (November 1, 2016) and the eutrophication model (December 31, 2016).
- Work with CHA, the consultant selected to assist Cornell with workplan tasks related to the outfall relocation and redesign, including:
  - Develop (engineers opinion of) costs for permitting, design, survey, bidding, construction
  - Identify potential suppliers and contractors; develop critical path timeline for acquisition of pipe and other materials.
  - Identify required regulatory permits and approvals from NYSDEC, ACOE, and any local municipalities; including SEQRA compliance
  - Identify required easements from Office of General Services
- Prepare a final report to NYSDEC.

## **6. Attachment: Technical Report**

---

# Technical Report: Calibration and Validation of Si3D for Cayuga Lake Modeling Project

April 25, 2016

Dr. Alexandra King

*Postdoctoral Associate, DeFrees Hydraulics Laboratory, School of Civil & Environmental Engineering, Cornell University, Ithaca, NY*

Prof. Edwin Cowen

*Professor & Director, DeFrees Hydraulics Laboratory, School of Civil & Environmental Engineering, Faculty Director for Energy, David R. Atkinson Center for a Sustainable Future, Cornell University, Ithaca, NY*

## 1. Improvements to the Diffuser Sub-model

In Status Report 1 (SR1), we proposed the following modification to eddy viscosity/diffusivity downstream of the LSC plume to obtain the linear spreading predicted by CORMIX II:

$$A_H = \alpha \sqrt{x - x_V} \exp\left(\frac{y^2}{B_{50}^2 (x - x_V)^2}\right)$$

Initial testing of this approach within Si3D produced linear spreading as desired, but we were unable to obtain convergence of the solution for an idealized test case, and application to Cayuga Lake presented questions about limits of the intermediate field.

We have since derived the exact form of  $A_H$  required in the intermediate field by the mass and momentum conservation equations for a multiport diffuser in shallow water.  $A_H = 0$  in the near field, where acceleration due to momentum injected at the diffuser dominates and lateral mixing is negligible by comparison, but the near-field region is short (distance  $0.5L_D$ ) where  $L_D$  is the diffuser length. The intermediate field, which follows immediately after the near field and persists until diffuser effects become negligible compared to background processes, is characterized by intense lateral mixing reflected in enhanced  $A_H$ . The intermediate field is divided into two regions: the zone of flow establishment (ZOFE), where the velocity profile takes a Gaussian shape outside a uniform-velocity potential core of width  $\delta(x)$ , and the zone of established flow (ZOEf), where the velocity profile is Gaussian.

Lee and Jirka (1980) derived the form of  $u_c(x)$ ,  $b(x)$ , and  $\delta(x)$  in these two regions, allowing for different entrainment coefficients  $\alpha_1$  and  $\alpha_2$  in the ZOFE and ZOEF, respectively. Lee and Jirka defined a dimensionless quantity to characterize the influence of friction: the far-field parameter  $\phi = C_D L_D / (2H)$  where  $C_D$  is the drag coefficient at the bed,  $L_D$  is the length of the diffuser, and  $H$  is the water depth. The following downstream coordinate, velocity, and half-width mark the end of the ZOFE and the beginning of the ZOEF:

$$x_I = \frac{L_D}{2\phi} \left[ \ln u_0 - \ln \left( 1 - \frac{(\sqrt{2} - 1)\phi}{2\alpha_1} \right) \right]$$

$$u_I = \sqrt{\frac{2m_0}{H}} \left( 1 - \frac{(\sqrt{2} - 1)\phi}{2\alpha_1} \right)$$

$$b_I = \frac{L_D}{2} \sqrt{\frac{2}{\pi}} \left( 1 - \frac{(\sqrt{2} - 1)\phi}{2\alpha_1} \right)^{-1}$$

where we have substituted the dimensionless function  $u_0(\phi)$  for an integral in Lee & Jirka. The approximation  $u_0(\phi) \approx 1.000 + 0.1890\phi + 0.0492\phi^2 + 0.0171\phi^3$  is correct within 0.0001 on the interval  $\phi = 0$  to 1 (for the LSC diffuser,  $\phi \sim 0.01$ , with the precise value depending on the bottom drag coefficient).

Substituting Lee and Jirka's solutions for  $u_c(x)$ ,  $b(x)$ , and  $\delta(x)$  into our formula for eddy viscosity/diffusivity, we obtain the following formula for horizontal eddy viscosity in the ZOFE past the acceleration zone ( $\frac{1}{2}L_D \leq x \leq x_I$ ) and outside the potential core ( $|y| > \delta(x)$ ):

$$\begin{aligned} A_H(x, y) &= \frac{1}{\sqrt{2}(\sqrt{2} - 1)} \alpha_1 u_c(x) b(x) \left( \frac{b(x)}{|y| - \delta(x)} \right) \left\{ \operatorname{erf} \left( \frac{|y| - \delta(x)}{b(x)} \right) \right. \\ &\quad \left. + \frac{1}{\sqrt{2}} \left[ e^{\left( \frac{|y| - \delta(x)}{b(x)} \right)^2} \operatorname{erfc} \left( \frac{|y| - \delta(x)}{b(x)} \right) - 1 \right] \right\} \end{aligned}$$

where

$$u_c(x) = \sqrt{\frac{2m_0}{H}} u_0 e^{-\frac{2\phi x}{L_D}}$$

$$b(x) = \frac{\alpha_1 L_D}{(\sqrt{2} - 1)\phi u_0} e^{\frac{2\phi x}{L_D}} \left( 1 - u_0 e^{-\frac{2\phi x}{L_D}} \right)$$

$$\delta(x) = \frac{L_D}{4u_0} e^{\frac{2\phi x}{L_D}} \left[ 1 - \frac{2\alpha_1}{(\sqrt{2} - 1)\phi} \left( 1 - u_0 e^{-\frac{2\phi x}{L_D}} \right) \right]$$

Note that  $A_H(x, y) \rightarrow 0$  as  $|y| \rightarrow \delta(x)$  and

$$A_H(x, y) \rightarrow \frac{1}{2} \alpha_1 u_c(x) b(x) \left( \frac{b(x)}{|y| - \delta(x)} \right)$$

as  $(|y| - \delta(x))/b(x) \rightarrow \infty$ . These limits must be programmed explicitly into Si3D because the formulas are sensitive to round-off error on a computer for large and small  $(|y| - \delta(x))/b(x)$ .  $A_H(x, y)$  is not defined in the potential core,  $|y| < \delta(x)$ , but we may set it to zero.

From Lee and Jirka's solutions we obtain the following formula for horizontal eddy viscosity in the ZOE (  $x > x_I$ ):

$$A_H(x, y) = \frac{1}{2} \alpha_2 u_c(x) b(x) \left( \frac{b(x)}{y} \right) \operatorname{erf} \left( \frac{y}{b(x)} \right)$$

where

$$u_c(x) = u_I e^{-\frac{2\phi}{L_D}(x-x_I)} \left[ 1 + \frac{8\alpha_2}{\sqrt{\pi}b_I} (x - x_I) \right]^{-1/2}$$

and

$$b(x) = b_I e^{\frac{2\phi}{L_D}(x-x_I)} \left[ 1 + \frac{8\alpha_2}{\sqrt{\pi}b_I} (x - x_I) \right]$$

Note that  $A_H(x, y) \rightarrow 0$  as  $y \rightarrow 0$ . This limit must be programmed explicitly into Si3D. In the near field, also called the "acceleration zone" ( $0 \leq x < \frac{1}{2}L_D$ ), it is assumed that  $A_H(x, y) = 0$ .

The values of  $A_H(x, y)$  discussed here are to be added to a uniform background value of  $A_H$  that may be used as a calibration parameter. This model introduces two additional parameters,  $\alpha_1$  and  $\alpha_2$ , that will be calibrated using the 2014 gridding data.

In Figure 1 and Figure 2 we plot  $A_H(x, y)$  in non-dimensional form for the LSC diffuser assuming bottom drag coefficient  $C_D = 0.002$  and entrainment coefficients  $\alpha_1 = \alpha_2 = 0.04$ . In both figures it can be seen that  $A_H$  approaches a constant value far from the source.

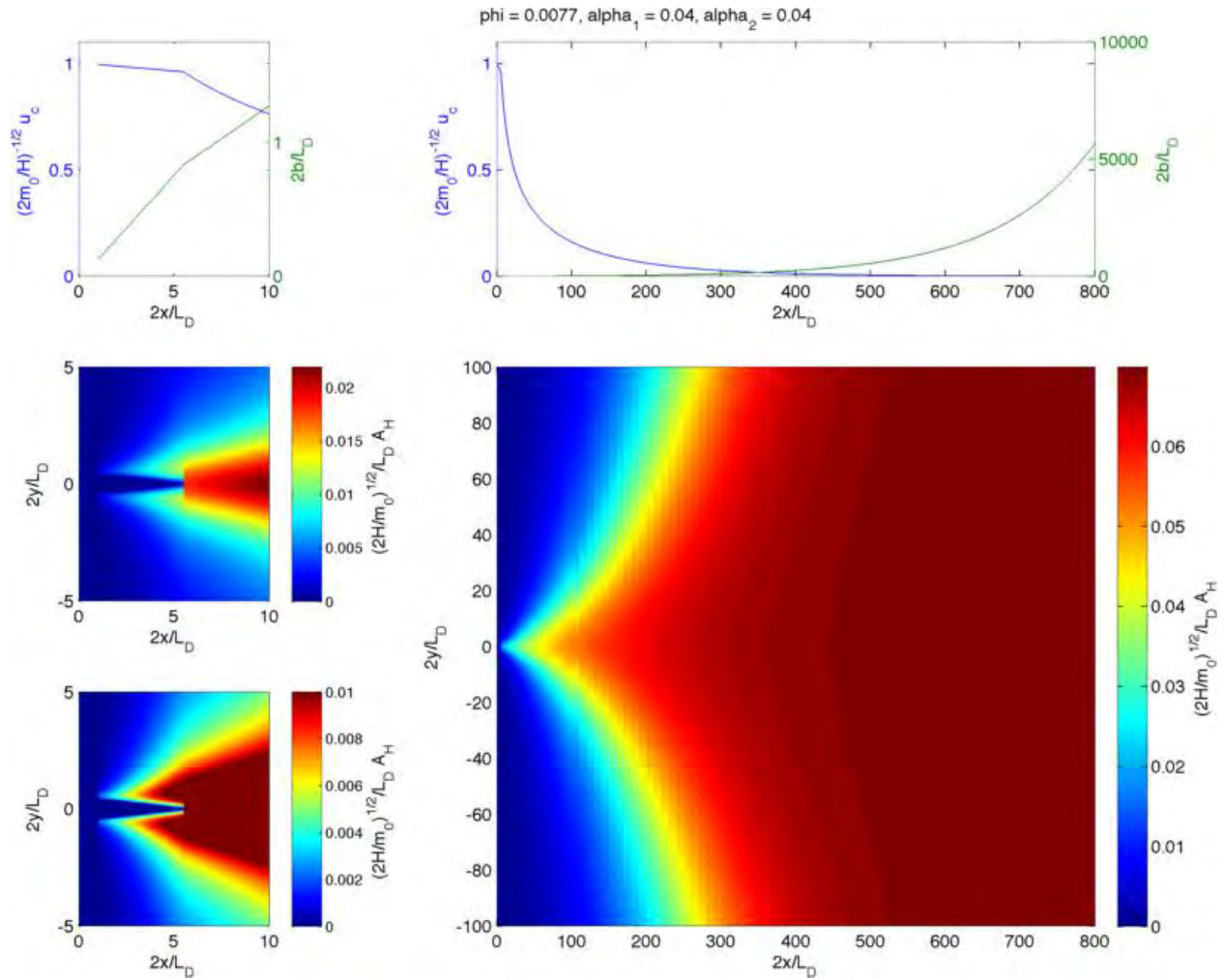


Figure 1. Plume predictions for far-field parameter  $\phi = 0.0077$  and entrainment coefficients  $\alpha_1 = \alpha_2 = 0.04$ . The top panels show centerline velocity and plume half-width as a function of distance downstream of the diffuser. The lower panels show horizontal eddy viscosity/diffusivity as a function of distance downstream and cross-stream from the diffuser. On the left we zoom in on the ZOFE, using two different scales for horizontal eddy viscosity/diffusivity.

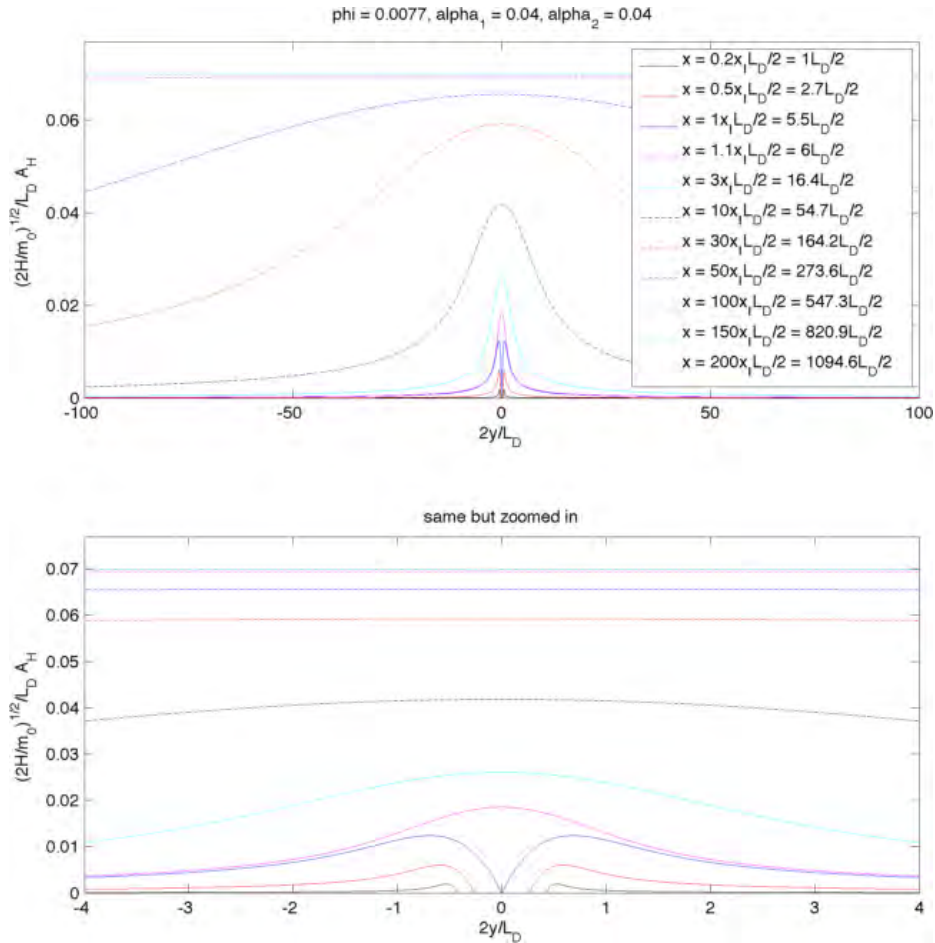


Figure 2. Plume predictions for far-field parameter  $\phi = 0.0077$  and entrainment coefficients  $\alpha_1 = \alpha_2 = 0.04$ .

## 2. Preliminary (Uncalibrated) Season-Long Simulations in 2012, 2013, and 2014

Although the diffuser model is not yet calibrated, we have set up season-long simulations for 2012, 2013, and 2014. These simulations will be re-executed once the final version of the code is ready. Here we describe the bathymetric grid, model drivers, and the data that will be used to test model performance. We also examine performance of the non-calibrated code, using the root mean square error (RMSE) metric to compare model predictions with measured temperatures and velocities.

### 2.1 Bathymetric Grid

The bathymetric grids provided to Si3D as input are plotted in Figure 3. First, low-resolution simulations of the entire lake are run to provide boundary conditions along the northern boundary of high-resolution simulations of the southern shelf. The low-resolution grid is 125m x

125m in the horizontal, and the high-resolution grid is 25m x 25m in the horizontal. The two grids employ the same vertical discretization, with grid cell depths varying between 0.5m for the surface cell to 2.9m for the bottom-most cell of the high-resolution grid and 4.4m for the bottom-most cell of the low-resolution grid.

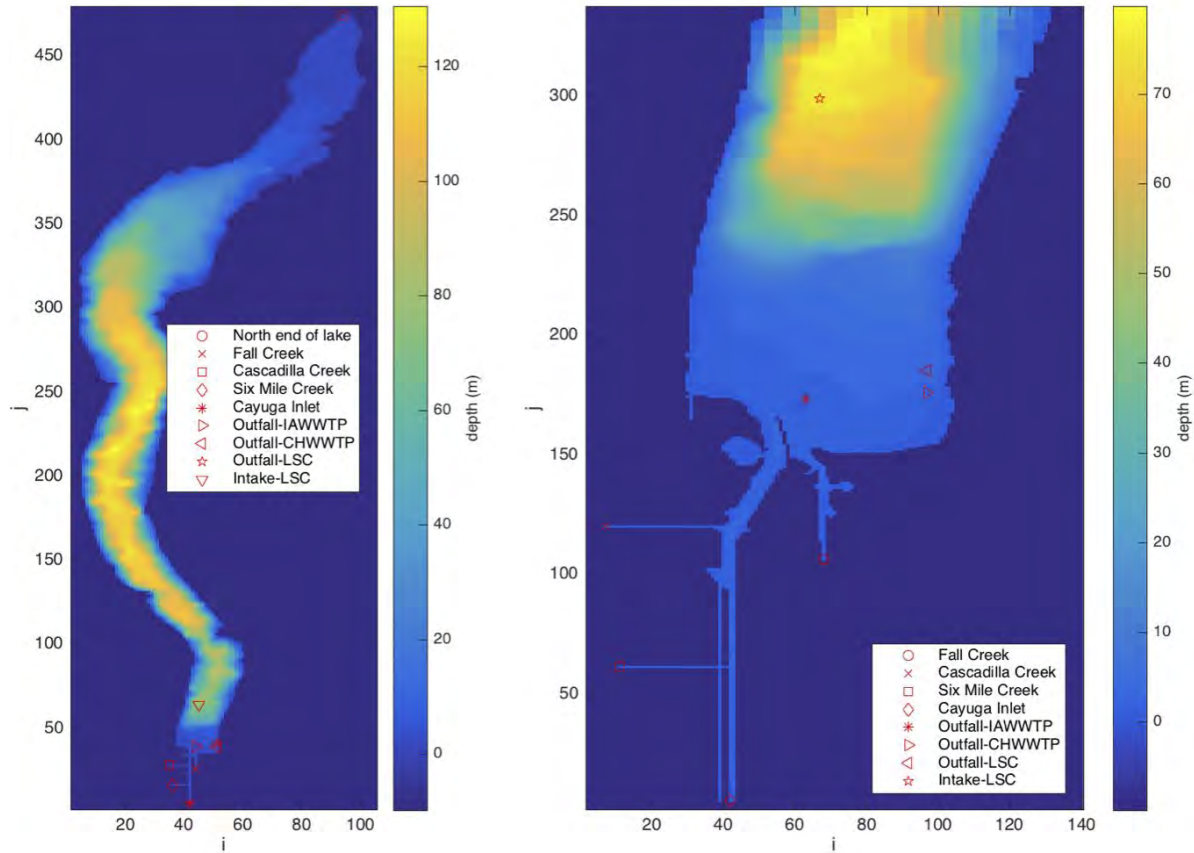


Figure 3. Bathymetric grids for low-resolution (left) and high-resolution (right) Si3D runs. Locations of open boundaries and point sources and sinks are indicated by red symbols. The entire northern edge of the high-resolution grid is also an open boundary, although it is not marked. Results from the low-resolution grid are used to specify the boundary condition along this northern boundary.

## 2.2 Model Drivers

Si3D simulations require (1) initial condition input consisting of a vertical temperature profile, and (2) time-dependent driver input that includes meteorological forcing at the surface and at the open boundaries, and point source/sink flow rates and temperatures. In this section, we discuss preparation of these input files and show values of the initial conditions and drivers for 2012, 2013, and 2014.

### 2.2.1 Initial Conditions

Si3D simulations are initialized with a temperature distribution that varies over depth and is uniform in horizontal planes. Our initial conditions are based on thermistor string data collected near the LSC intake. Internal wave amplitudes are strong at the intake thermistor string site, so to obtain an initial temperature profile representative of the entire lake, we take a 5-day thermocline-centered average of temperature about the simulation start time (5 days is equal to about two internal wave periods). The elevation of the thermocline,  $z_T$ , is defined as the average elevation weighted by the temperature gradient:

$$z_T = \frac{\int_0^H z \frac{dT}{dz} dz}{\int_0^H \frac{dT}{dz} dz}$$

where  $T$  is temperature,  $z$  is elevation,  $z = 0$  is the elevation of the bed, and  $z = H$  is the elevation of the water surface. Thermocline elevation is more commonly defined as the elevation of the maximum temperature gradient, but we found this definition to be highly sensitive to transient (lasting several hours or less) pronounced temperature gradients near the water surface. The gradient-weighted depth average definition is more robust, yielding elevations similar to the more common definition under average conditions without the sensitivity to transient surface gradients.

Our initial conditions for 2012, 2013, and 2014 are plotted in Figure 4. Simulation start dates are listed in the figure legend.

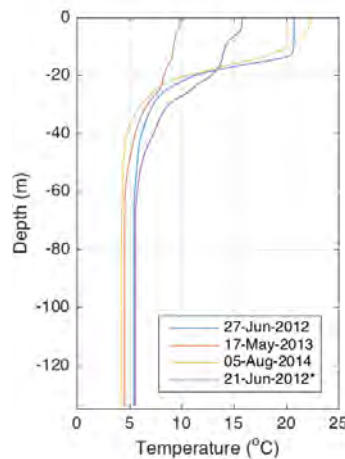


Figure 4. Initial conditions for 2012, 2013, and 2014 simulations. The earlier 2012 initial condition (marked with “\*”) was used for a short simulation to compare to ADCP velocity data.

### 2.2.2 Surface Boundary Conditions

Surface boundary conditions for the 2012, 2013, and 2014 simulations are plotted in Figure 5. Heat flux and wind stress must be specified at the water surface. Si3D calculates these from shortwave radiation, air temperature, atmospheric pressure, relative humidity, cloud cover, wind drag coefficient, and wind vector components, which are provided as time-dependent

input. Additionally, the light extinction coefficient must be specified so Si3D can appropriately distribute solar heat inputs over the water column.

The meteorological station at the piling cluster measures shortwave radiation, air temperature, atmospheric pressure, relative humidity, wind speed, and wind direction every 10 minutes. Wind is measured 8m above the water surface — we multiply measure wind speed by  $(10/8)^{1/7}$  to obtain wind speed 10m above the water surface. We compute wind drag coefficient using the method recommended by Wüest and Lorke (2003). Cloud cover is estimated from the difference between measured shortwave radiation and the shortwave radiation expected on a clear day.

Light extinction coefficient ( $K_d$ ) was measured every two weeks in 2013 at the LSC sampling sites, and we use these Site 3 measurements to drive the model in 2013. In 2012 and 2014, however, we do not have measurements of  $K_d$  — in 2012 we have Secchi depth measurements from which we may calculate  $K_d$ , but in 2014 we have no measurements of  $K_d$  or Secchi depth, so we must use historical values.

UFI measured  $K_d$  at Site 3 (formerly called “LSC Site 8”) on a biweekly basis during the stratified season from 1998 to 2006 and in 2013; from these measurements we compute a biweekly median  $K_d$ , which is plotted along with biweekly mean and standard deviation in Figure 6. To clarify, the median, mean, and standard deviation were computed across all years at each two-week interval. We use the time-dependent median  $K_d$  to drive the 2014 simulation.

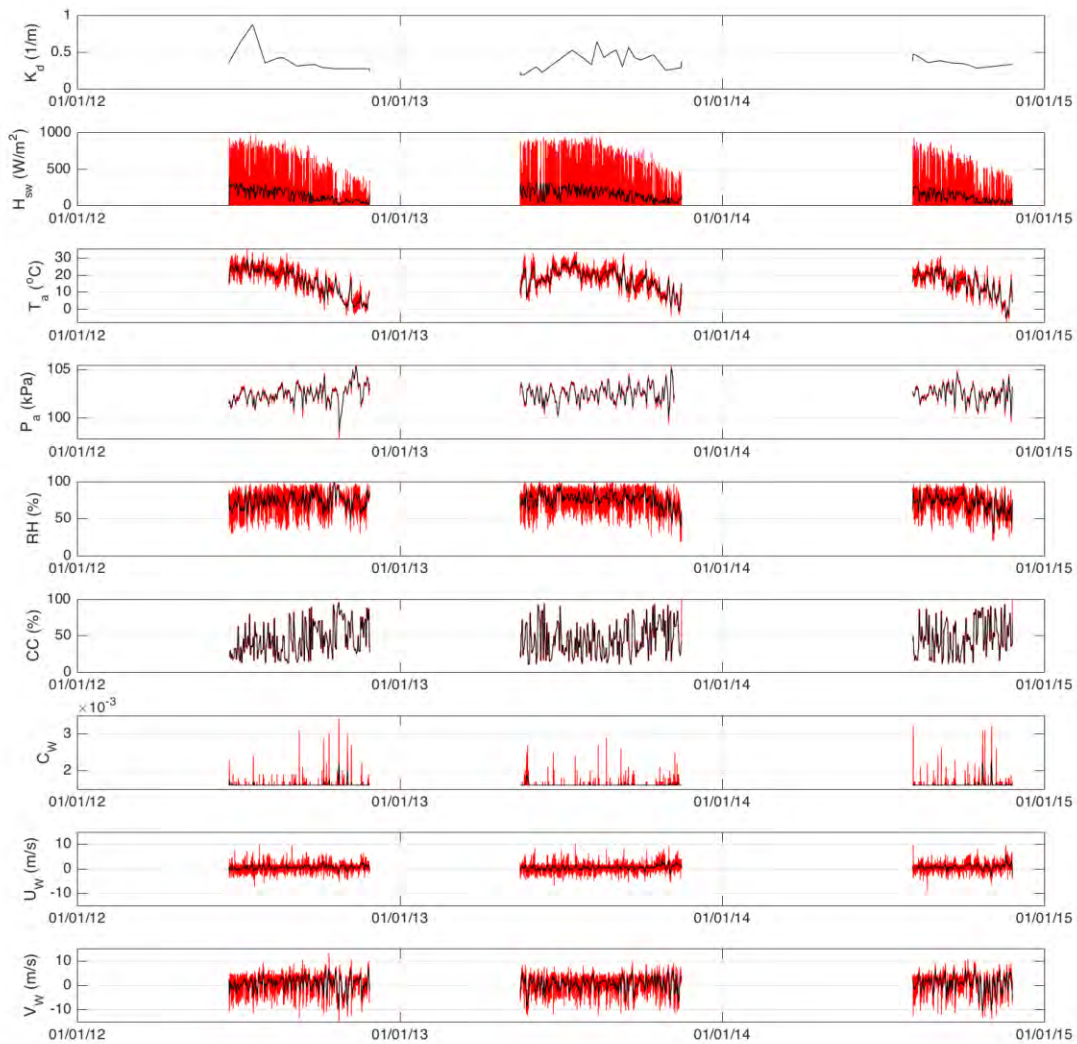


Figure 5. Surface boundary conditions for 2012, 2013, and 2014 simulations. The 10-min measurements used to drive the simulations are shown in red and a 1-day moving average is overlaid in black for better legibility. Time histories include light extinction coefficient ( $K_d$ ), shortwave radiation ( $H_{sw}$ ), air temperature ( $T_a$ ), atmospheric pressure ( $P_a$ ), relative humidity (RH), cloud cover (CC), wind drag coefficient ( $C_w$ ), and wind speed components ( $U_w, V_w$ ). Wind speed components represent east and north directions with respect to the bathymetric grid, which is rotated relative to true north.

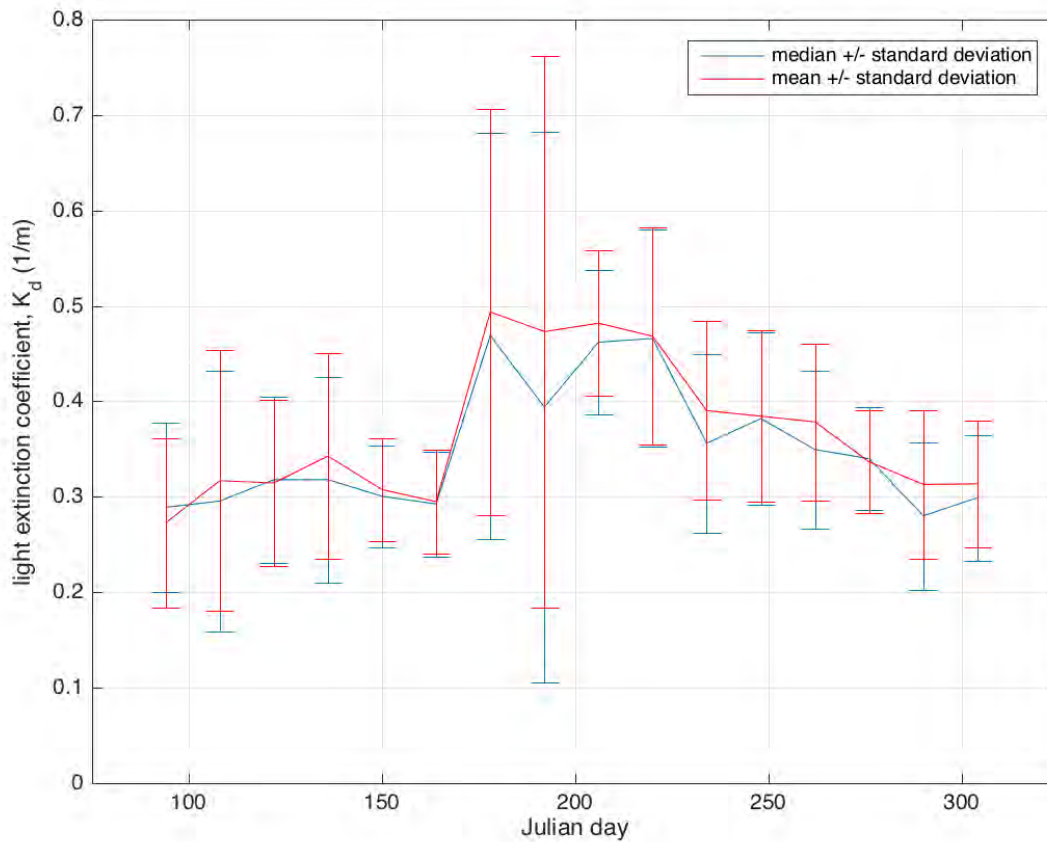


Figure 6. Statistics of light extinction coefficient,  $K_d$ , measured by UFI at Site 3 (previously “Site 8”), biweekly from 1998–2006 and also in 2013. Mean, median, and standard deviation are computed over all years at two-week intervals.

For the 2012 simulation, we use the estimate

$$K_d = 0.84 (SD)^{-1} + (0.16)m^{-1}$$

where  $SD$  is Secchi depth measured at Site 3, to compute extinction coefficients for driving the model. This linear relationship is based on a regression by UFI for their biweekly Site 3 data (1998–2006 plus 2013). The relationship between  $K_d$  and  $(SD)^{-1}$  is not particularly strong ( $R^2 = 0.57$ ), which UFI notes is “supported by general optical theory and UFI’s analysis of Cayuga Lake’s in situ optical properties”, in that the ratio of absorption-to-scattering varies over time and between sampling sites within Cayuga Lake,  $K_d$  is influenced more by absorption than by scattering, and Secchi depth is influenced more by scattering than by absorption [personal communication with Susan O’Donnell]. See Figure 7 for a comparison of  $K_d$  estimates from Secchi depth in 2012 to statistics of directly measured  $K_d$ .

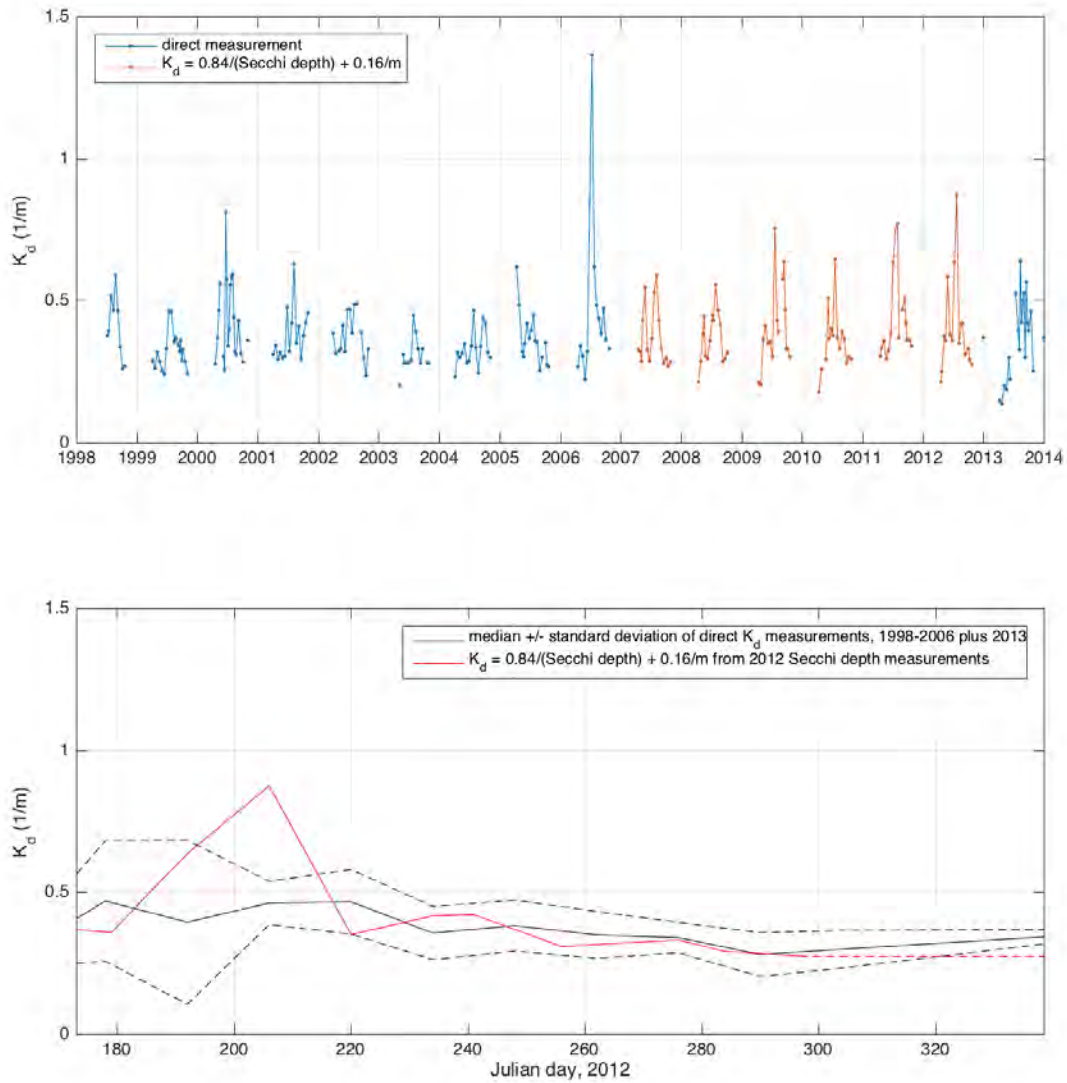


Figure 7. Time history showing, in top panel, light extinction coefficient measured by UFI at Site 3 (formerly Site 8) from 1998–2006 and 2013 as well as light extinction coefficient estimated by Cornell’s Secchi depth measurements at Site 3 from 2007–2012. The lower panel shows estimates of  $K_d$ , based on measurements of Secchi depth at Site 3, used to drive 2012 simulations. Note that Secchi depth was not measured after day 296, and the dashed red line shows extrapolated values. Also plotted, for reference, is the median and median  $\pm$  one standard deviation of all UFI’s measurements of  $K_d$  at Site 3 from 1998–2006 plus 2013.

### 2.2.2 Open Boundary Conditions

Open boundary conditions: flow rate, temperature, and water surface elevation time histories, used to drive the season-long simulations are plotted in Figure 8.

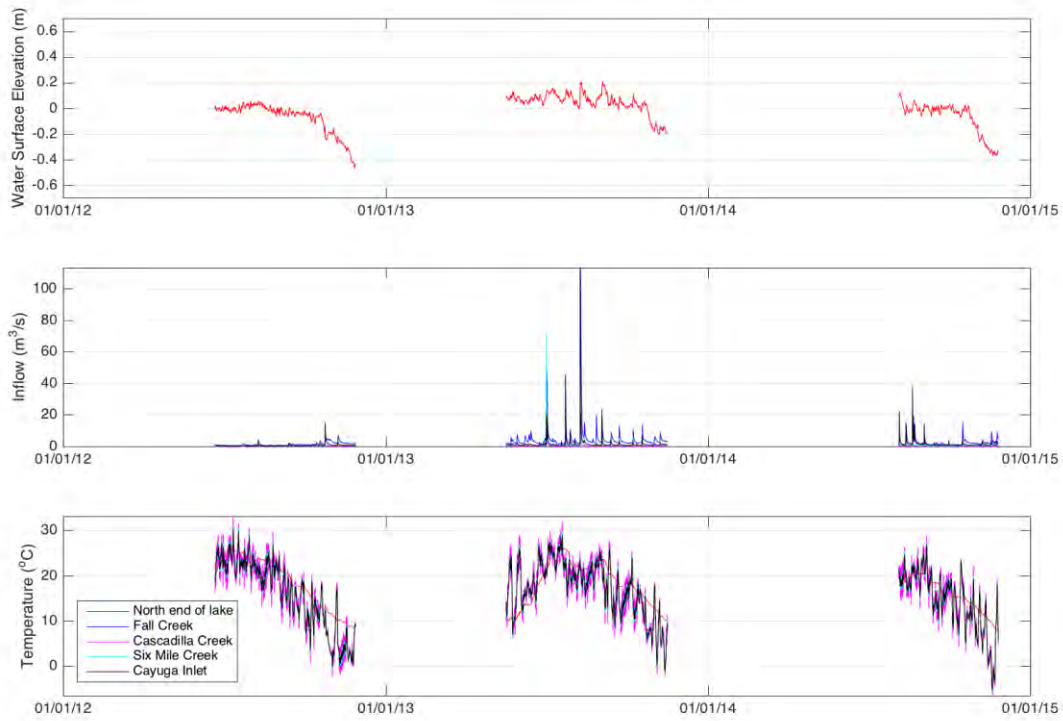


Figure 8. Open boundary conditions for 2012, 2013, and 2014 simulations. Water surface elevation (referenced to 116.6m above NGVD1929) is specified at the north end of the lake and flow rate is specified at the tributaries.

### 2.2.3 Point Sources and Sinks

Point source and sink flow rates and temperatures used to drive the season-long simulations are plotted in Figure 9.

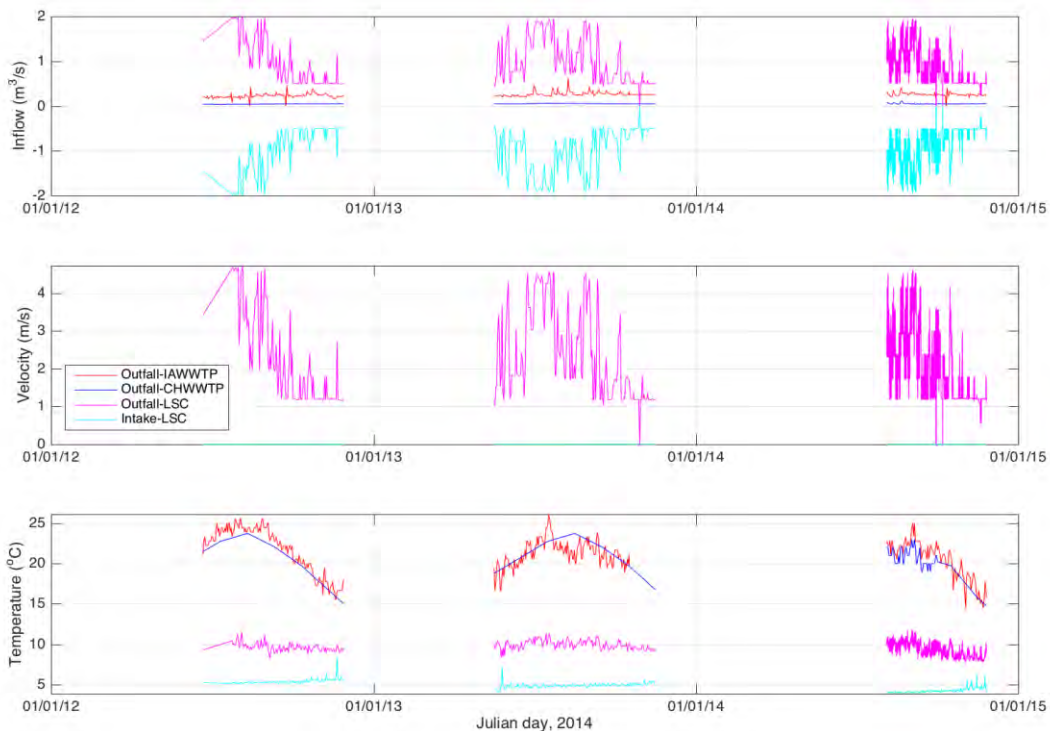


Figure 9. Point source and sink time series used to force 2012, 2013, and 2014 simulations.

### 2.3 Data Used to Test Model Performance

Model performance will be evaluated by comparing model predictions to the following field data:

1. Water temperature at a depth of 2m at the Piling Cluster. These measurements were recorded every 15min in 2012, 2013, and 2014 in addition to other years
2. Water temperatures at the LSC intake site, in ~80m of water, measured at depth intervals of several meters from the surface to below the thermocline. Measurements were recorded every 1-2min in 2012, 2013, and 2014
3. ADCP velocity profile data recorded in ~25m of water near the east shore off Millikan Point during a short experiment in 2012
4. Gridding data from 2014 – this data will be used to calibrate and validate the diffuser sub-model

In this report, we show preliminary results comparing to data sources 1 – 3 only.

## 2.4 Model Performance

### 2.4.1 Temperatures at the Piling Cluster and the LSC Intake Site

In Figure 10, Figure 11, and Figure 12, we compare measured and modeled temperatures at the piling cluster and LSC intake site. RMSE is computed as a 2-day rolling average and plotted in the final panel of each figure for the piling cluster, for each thermistor on the LSC intake thermistor string, and as a depth-average for the intake thermistor string data. The depth averaged RMSE is computed by integrating the mean square error over depth, dividing by total depth, and then taking the square root. Piling cluster and depth-averaged intake site RMSE is always under 3°C and more typically in the 1-2°C range. Si3D captures significant qualitative features of the spatio-temporal temperature field including upwelling events (e.g., day 218 in 2012, day 192 in 2013, and day 224 in 2014) and other periods of intense internal wave activity (e.g., day 255-263 in 2014).

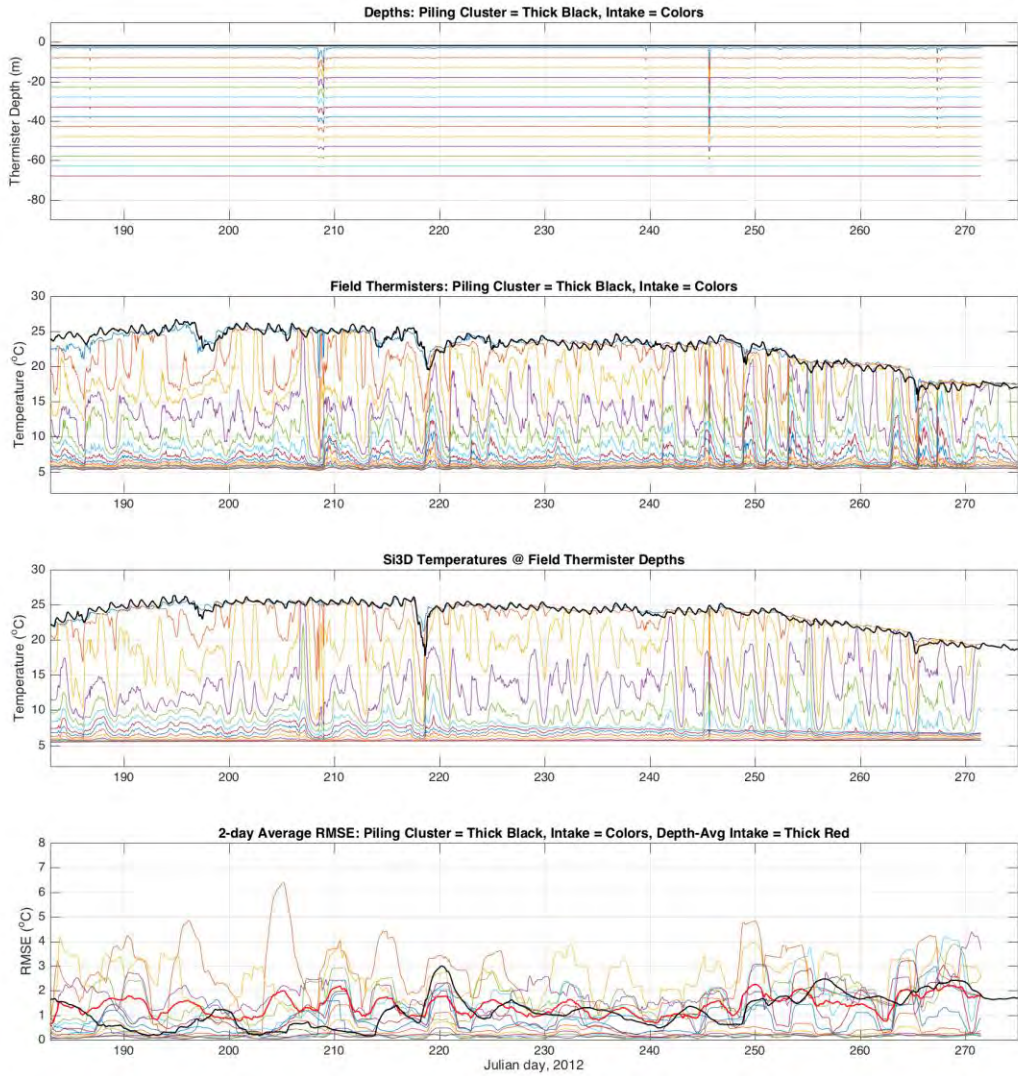


Figure 10. Comparison of measured and modeled temperature data for 2012. Piling cluster data is plotted with a thick black line. Thermistor depths are plotted in the top panel; the second panel shows temperatures measured at those depths in the field; the third panel shows temperatures predicted at those depths by Si3D; in the final panel we show a rolling RMSE computed over a 2-day averaging window. RMSE is shown for the piling cluster (thick black line), for each of the thermistors on the LSC intake thermistor string (colored thin lines), and the depth-averaged RMSE for the LSC intake thermistor string (thick red line).

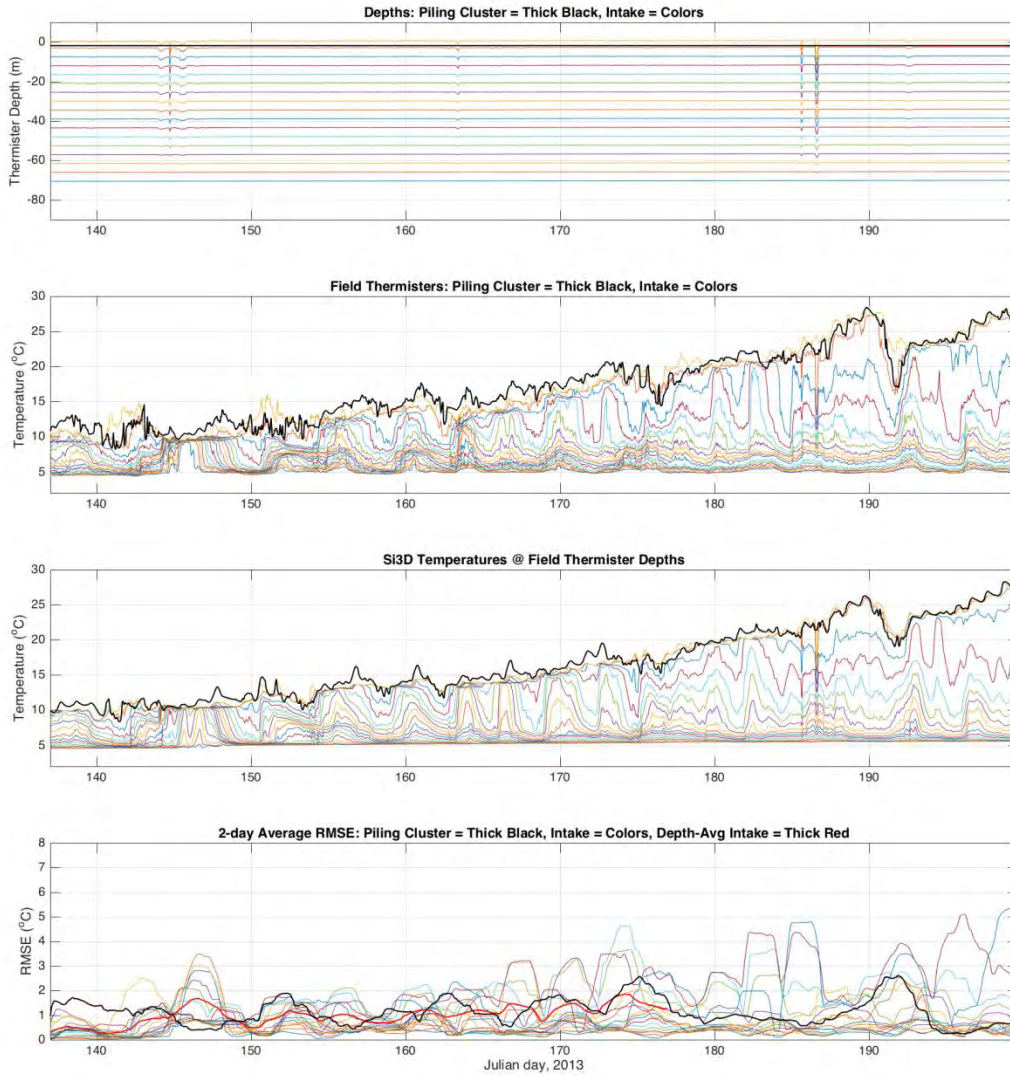


Figure 11. Comparison of measured and modeled temperature data for 2013. Piling cluster data is plotted with a thick black line. Thermistor depths are plotted in the top panel; the second panel shows temperatures measured at those depths in the field; the third panel shows temperatures predicted at those depths by Si3D; in the final panel we show a rolling RMSE computed over a 2-day averaging window. RMSE is shown for the piling cluster (thick black line), for each of the thermistors on the LSC intake thermistor string (colored thin lines), and the depth-averaged RMSE for the LSC intake thermistor string (thick red line).

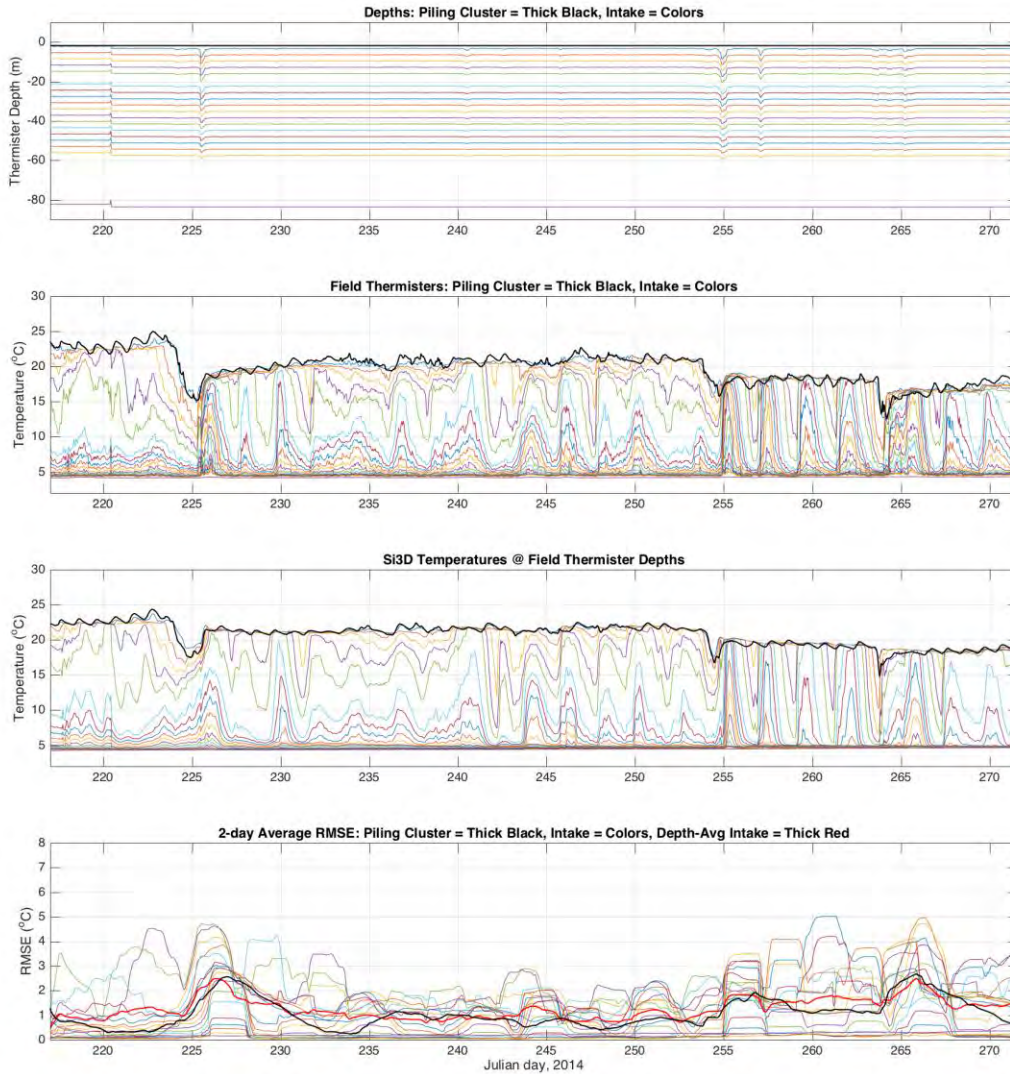


Figure 12. Comparison of measured and modeled temperature data for 2014. Piling cluster data is plotted with a thick black line. Thermistor depths are plotted in the top panel; the second panel shows temperatures measured at those depths in the field; the third panel shows temperatures predicted at those depths by Si3D; in the final panel we show a rolling RMSE computed over a 2-day averaging window. RMSE is shown for the piling cluster (thick black line), for each of the thermistors on the LSC intake thermistor string (colored thin lines), and the depth-averaged RMSE for the LSC intake thermistor string (thick red line).

#### 2.4.2 Velocity Profile in 2012

We ran a short simulation starting earlier in 2012, before we were able to take a full 5-day average of the available thermistor string data to obtain the initial condition, so we could compare to ADCP data collected off Millikin Point in about 25m of water for a 10-day period. Model results are compared to the field measurements in Figure 13. The 2-day rolling average, depth-averaged RMSE is below 0.1m/s during the entire deployment, and Si3D reproduces

observed large-amplitude velocity oscillations due to internal waves despite the short initialization period.

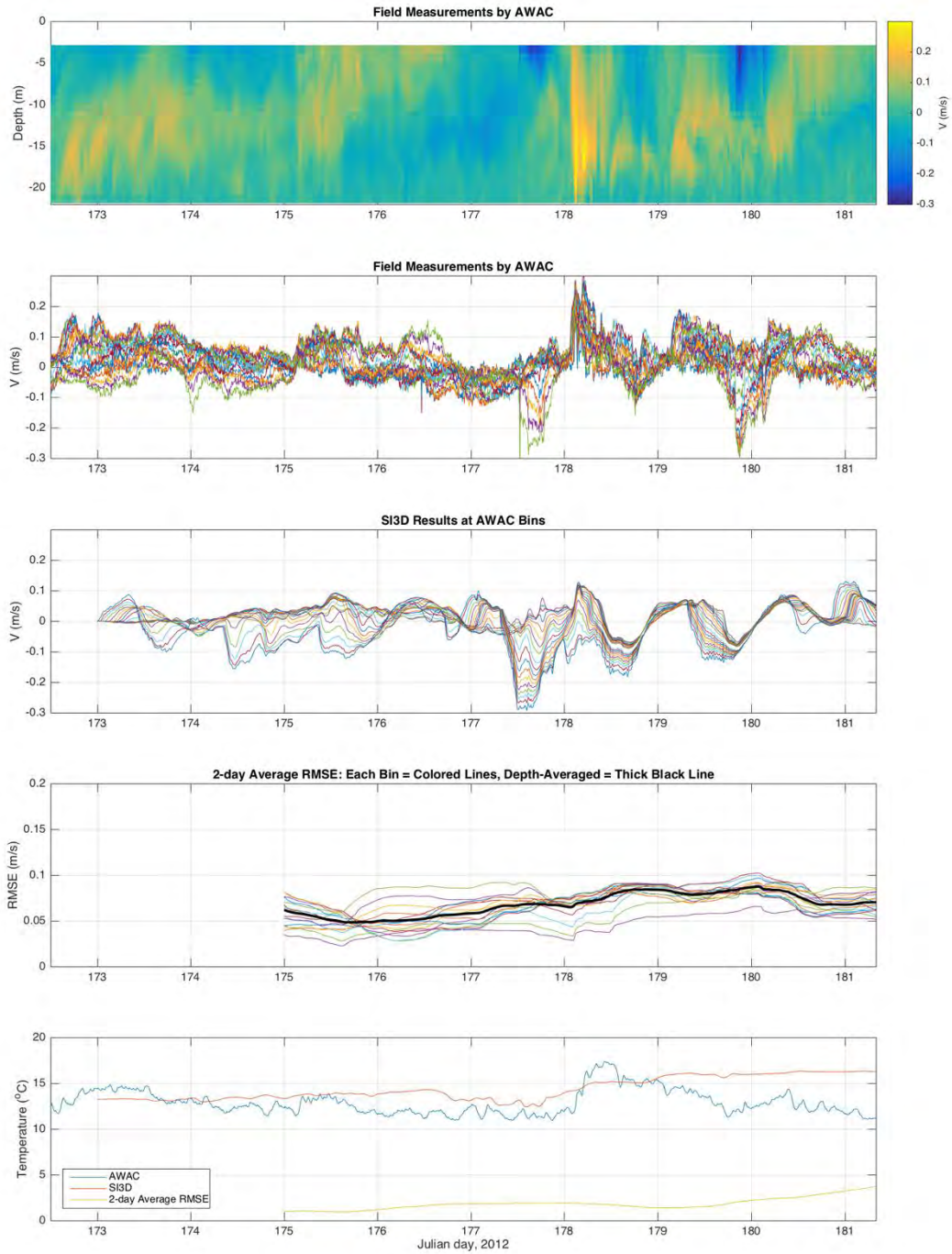


Figure 13. Comparison of measured and modeled ADCP data for 2012.

### 3. Sensitivity Analysis and Initialization Options

A preliminary sensitivity analysis was performed using the first 27 days of the 2014 simulations. This shorter time period was used to reduce computational cost. Note that for these simulations, we failed to adjust the wind speed to a 10m height, so wind speeds and drag coefficients driving the code are slightly in error, but otherwise, initial conditions, boundary conditions, and point source inputs are the same as described in the previous section. In this section we also examine the possibility for initializing simulations before temperature profile data is available.

#### 3.1 Reference Simulation

We compare all sensitivity tests to a reference simulation. For the reference simulation, the bed drag coefficient was set to  $C_D = 0.002$ , and background horizontal eddy viscosity was set to  $A_H = 1.0 \text{ m}^2/\text{s}$ . Wind drag coefficient,  $C_D$ , and light extinction coefficient,  $K_d$ , were specified as described in the previous Section 2.2.2. In Figure 13 we compare field measurements and Si3D predictions for this reference simulation.

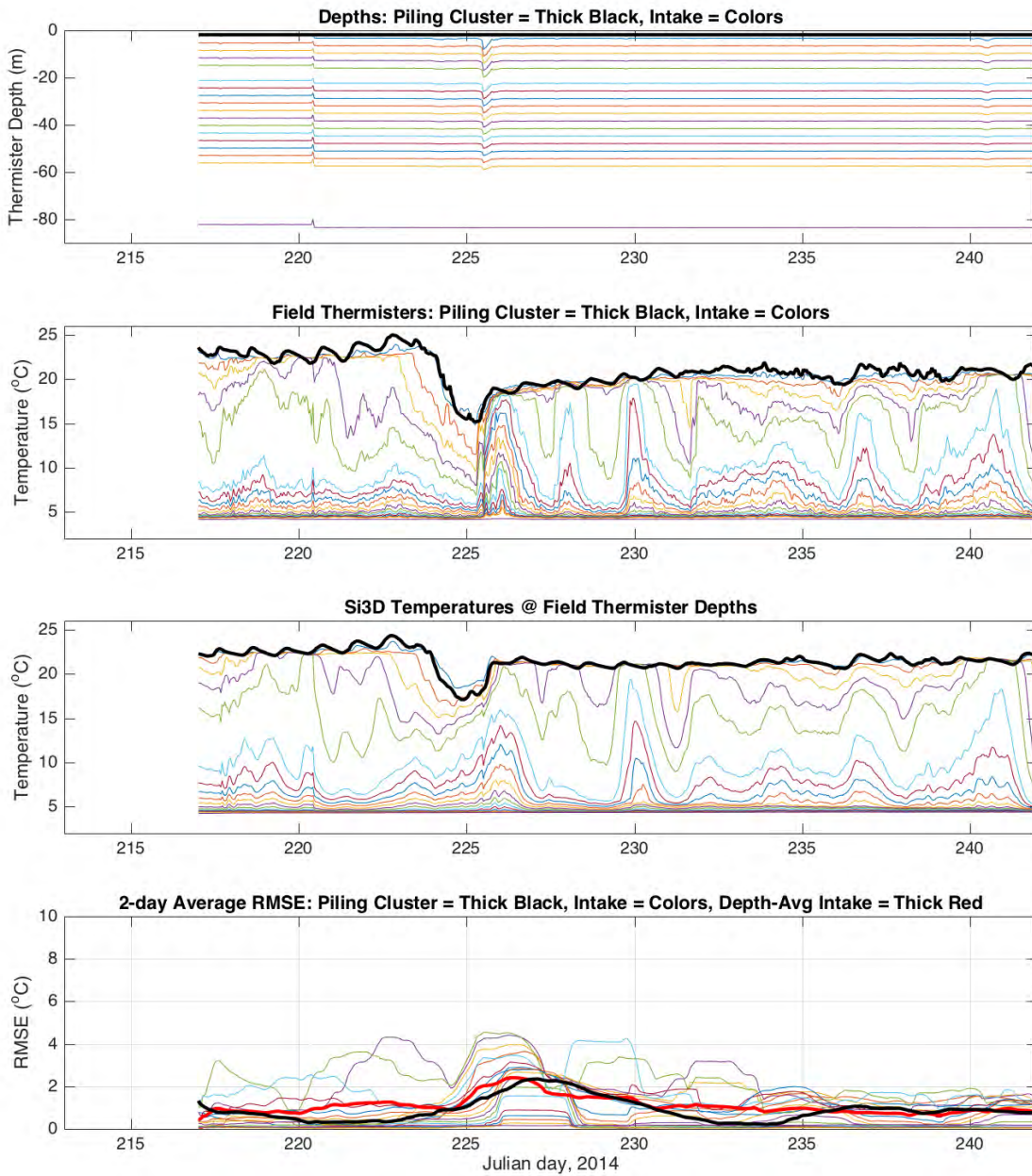


Figure 14. Comparison of measured and modeled temperature data for reference simulation used for sensitivity analysis.

### 3.2 Sensitivity to extinction coefficient, horizontal eddy viscosity, drag coefficients, and grid resolution

In our first sensitivity test, tested three different values of  $K_d$  and three different values of  $A_H$ , running simulations for all nine combinations of these parameters. While in the reference simulation,  $K_d$  varied in time,  $K_d$  was constant in these simulations. The three values of each parameter were chosen to span the range of physically reasonable values. Simulation results

(RMSE from comparison of piling cluster and intake thermistor string temperatures) are compared to the reference simulation in Figure 15 after both the low-resolution runs and the high-resolution runs. The difference between high-resolution and low-resolution results is imperceptible. The model results show some sensitivity to both  $K_d$  and  $A_H$ . The two higher values of  $K_d$  slightly improve model performance measured by the maximum (over depth) RMSE at the intake site, but make little improvement or hurt model performance for piling cluster temperatures and intake site temperatures when performance at the intake site is measured by depth-averaged RMSE. Changing  $A_H$  has little effect except at the highest value, in which case it hurts performance by all measures. Overall, temperature predictions at the intake site and the piling cluster are not very sensitive to  $K_d$  or  $A_H$ . A similar experiment modifying wind drag coefficient,  $C_W$ , and bed drag coefficient,  $C_D$ , (results shown in Figure 16) leads to a similar conclusion: there is negligible difference between high-resolution and low-resolution results and modifying drag coefficients offers little or no improvement to model predictions.

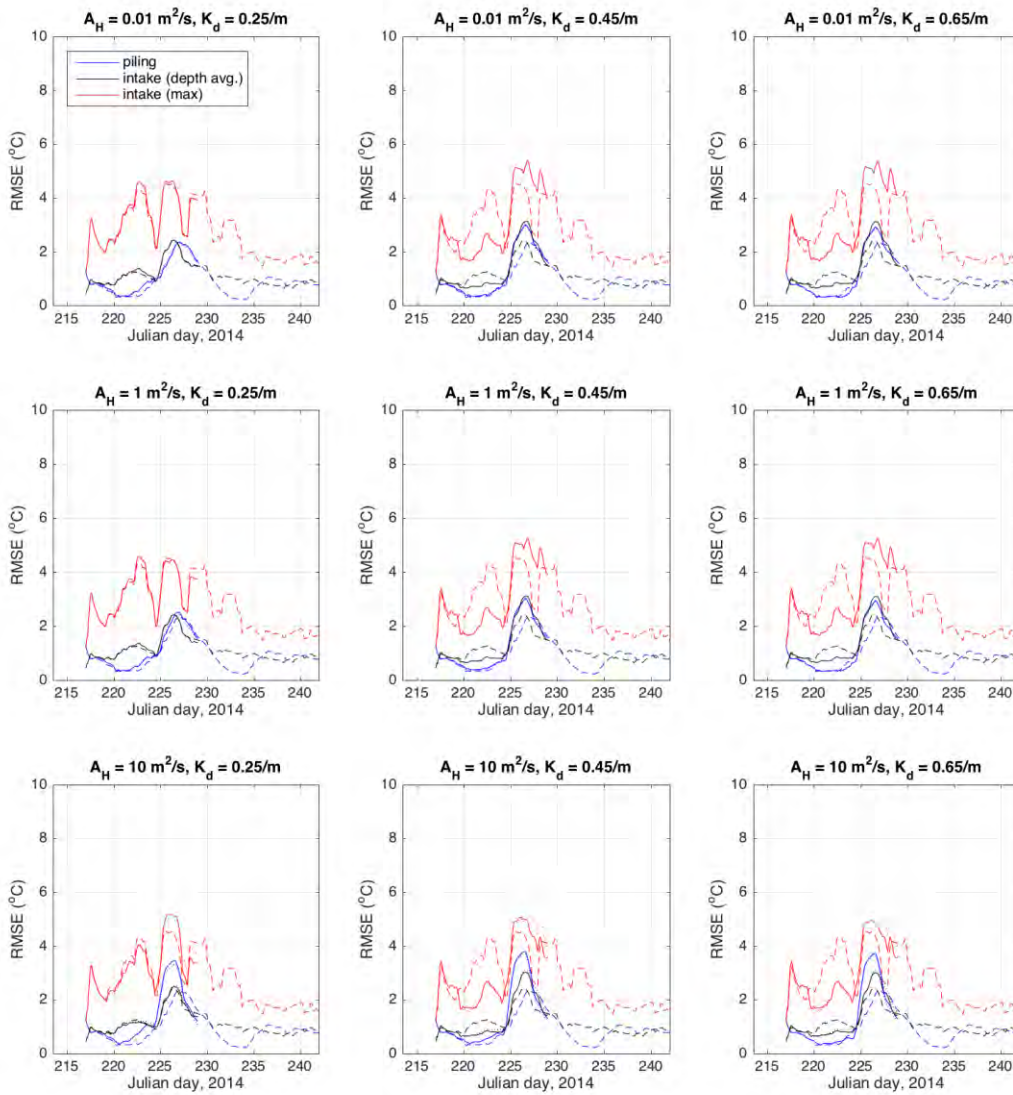


Figure 15. Test of sensitivity to horizontal eddy viscosity ( $A_H$ ), light extinction coefficient ( $K_d$ ), and grid resolution. Root mean square error (RMSE) is a 2-day running average, comparing field data to simulation. Results for reference simulation are plotted as a dashed line in each window for comparison. RMSE for piling cluster is in blue, depth-averaged RMSE for intake thermistor string is in black, and maximum RMSE for intake thermistor string is in red. Results of low-resolution runs are plotted as solid lines, and results of high-resolution runs are plotted as dotted lines. The high-resolution and low-resolution results are usually identical, thus the dotted lines are rarely visible.

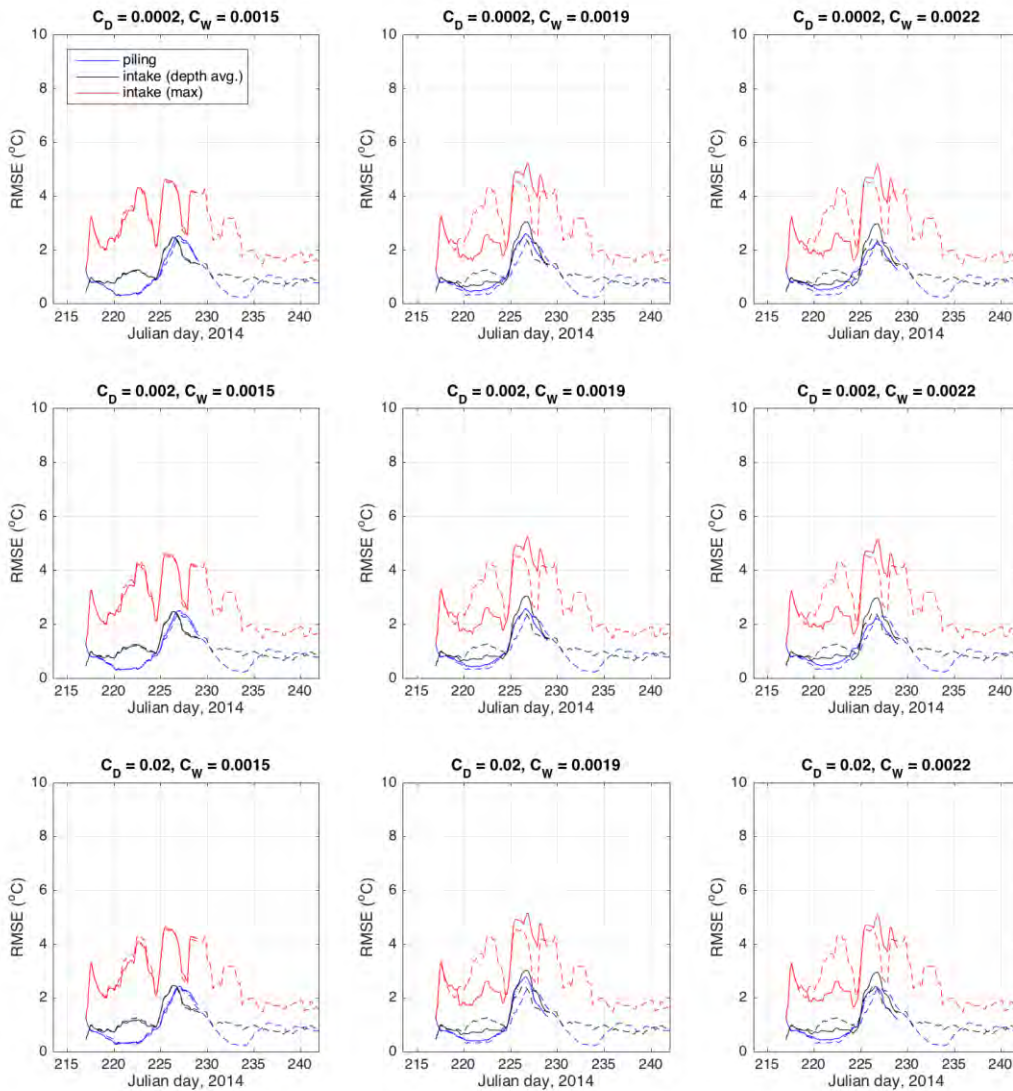


Figure 16. Test of sensitivity to bed drag coefficient ( $C_D$ ), wind drag coefficient ( $C_W$ ), and grid resolution. Root mean square error (RMSE) is a 2-day running average, comparing field data to simulation. Results for reference simulation are plotted as a dashed line in each window for comparison. RMSE for piling cluster is in blue, depth-averaged RMSE for intake thermistor string is in black, and maximum RMSE for intake thermistor string is in red. Results of low-resolution runs are plotted as solid lines, and results of high-resolution runs are plotted as dotted lines. The high-resolution and low-resolution results are usually identical, thus the dotted lines are rarely visible.

### 3.3 Sensitivity to initial condition and simulation start time

Using a measured temperature profile to initialize Si3D means that the model cannot be run before temperature measurements are available in a given year. This is restrictive, and we tested an alternative approach: using non-dimensional temperature profiles along with continuous temperature measurements available from the piling cluster and the LSC heat-

exchange facility to construct initial conditions. We may define a non-dimensional temperature profile as follows:

$$T^*(z^*) = \frac{T(z) - T_{IN}}{T_{PC} - T_{IN}}$$

where  $T^*(z^*)$  is the dimensionless profile,  $T(z)$  is the dimensional temperature profile,  $T_{PC}$  is the temperature at the piling cluster, and  $T_{IN}$  is the temperature of the intake water measured at the LSC heat-exchange facility. Elevation,  $z$ , is defined to be zero at the water surface and negative below the surface. Dimensionless elevation is defined as

$$z^* = \frac{z + H_E}{H_E}$$

where  $H_E$  is the epilimnion depth, defined as the distance from the water surface to the thermocline. We computed dimensionless temperature profiles in 2013 because the intake thermistor string was deployed early in that year. To re-dimensionalize the 2013 temperature profiles for initializing the 2014 simulations, after May 14 (day 135) we had to choose an epilimnion depth (on day 135 and earlier in 2013 a thermocline was not present), and we do not know the epilimnion depth before we have temperature profile measurements in 2014. Thus we guessed three epilimnion depths: the epilimnion depth from the corresponding day of the year in 2013 +/- 5m. In Figure 17 we show the resulting dimensional temperature profiles used to initialize the 2014 simulations at nine earlier start dates, and in Figure 18 and Figure 19 we compare the performance of these simulations to that of the reference simulation. Initializing the simulation with a nearly-uniform profile on day 121 (April 30) produces results that are worse than those in the reference simulation but not terrible. The results of simulations initialized once the lake is stratified are highly sensitive to epilimnion depth, and while none of the simulations performs better than the reference simulation, some of the model results for simulations initialized later in the year perform as well as the reference simulation. These results suggest that this method could be used to fill in the gaps where temperature profile data are not available early in a given year, so long as temperature profile data are available later in the year to verify the initial condition. Motivated by these results, we tested more epilimnion depths for the later dates. The initial conditions are shown in Figure 20 and the results are shown in Figure 21, Figure 22, and Figure 23. In these simulations, with a good choice of epilimnion depth, we were again able to obtain results as good as but not better than the reference simulation.

In summary, Si3D temperature predictions are highly sensitive to initial conditions. Initializing a simulation early in the season with uniform temperature profile may produce satisfactory results, and it is possible to initialize a simulation during the stratified season but before temperature profile data is available provided that there are temperature profile data available later in the season to verify the initial condition.

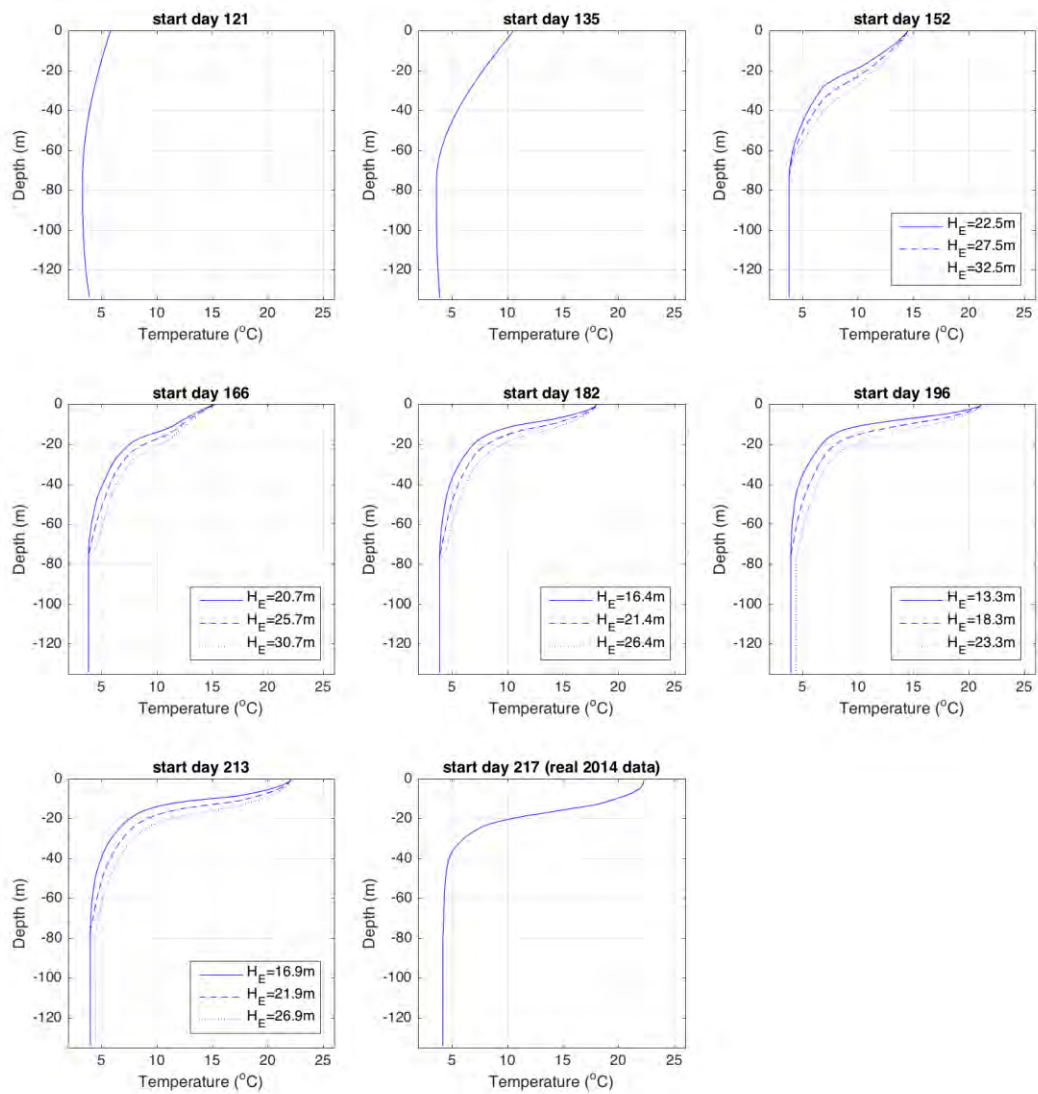


Figure 17. Initial conditions used to test sensitivity to starting date of simulation. These are based on non-dimensional temperature profiles from 2013 obtained from the same day of the year, and they are dimensionalized using 2014 measurements of 12-day average temperature at the piling cluster and at the intake for the LSC plant. When the non-dimensional temperature profile includes a well-defined thermocline, we must also specify an epilimnion depth  $H_E$  to obtain a dimensional profile. We do not have measurements of epilimnion depth in 2014, so we used three guesses: the epilimnion depth measured on the same day in 2013 and that value  $\pm 5m$ . The resulting initial conditions based on these three values of  $H_E$  are plotted in the same window, where applicable. The default initial condition, which is based on real 2014 thermistor string measurements near the LSC intake, is plotted in the last panel.

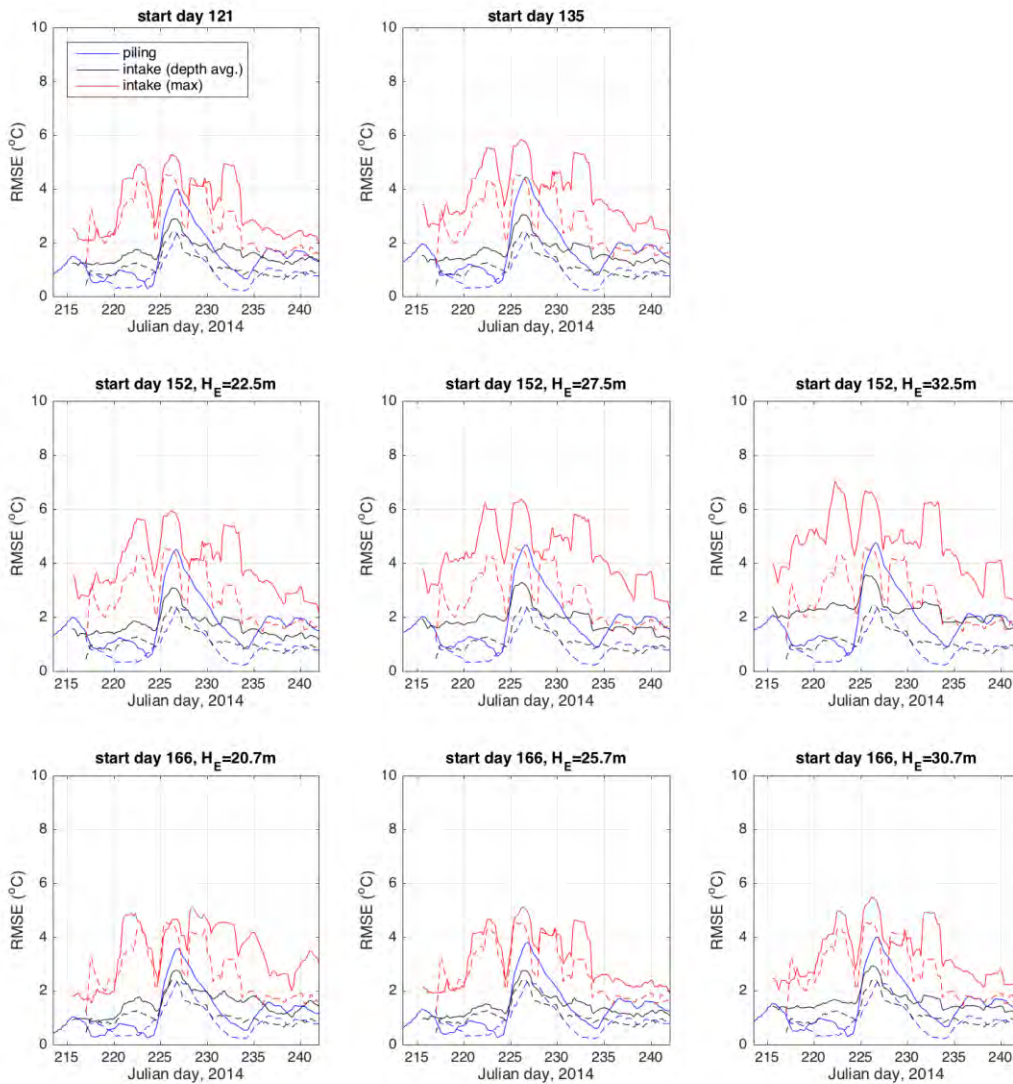


Figure 18. Test of sensitivity to simulation start date and initial condition. Root mean square error (RMSE) is a 2-day running average, comparing field data to simulation. Results for reference simulation are plotted as a dashed line in each window for comparison. RMSE for piling cluster is in blue, depth- averaged RMSE for intake thermistor string is in black, and maximum RMSE for intake thermistor string is in red. No high resolution runs were conducted – all results are for low resolution runs. The reference simulation was initialized with real temperature data on day 217. The rest of the simulations were initialized using re-scaled temperature profiles measured 2013, with a varying epilimnion depth. The initial conditions corresponding to these simulations are plotted in Figure 1.12. Results for more dates are plotted in Figure 19.

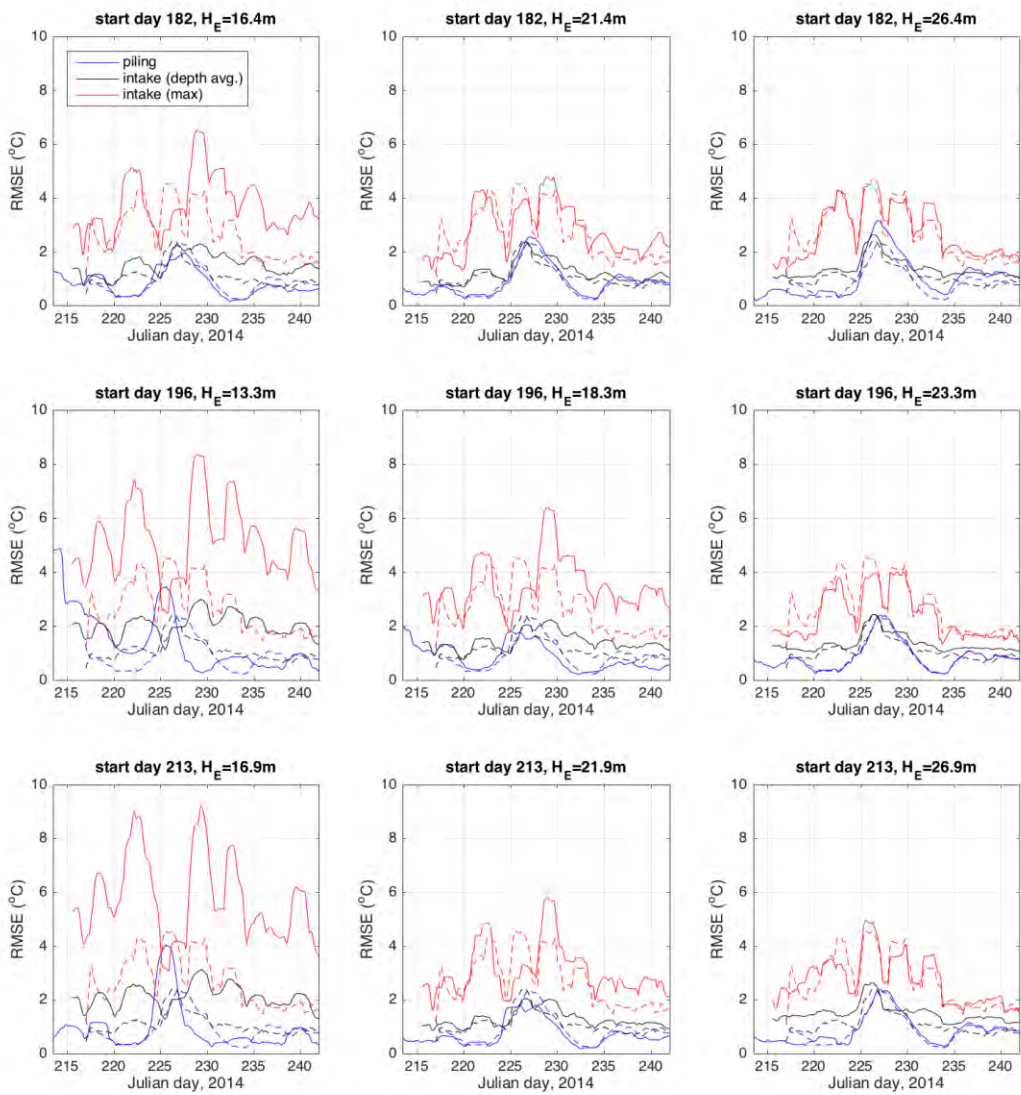


Figure 19. Figure 18, continued.

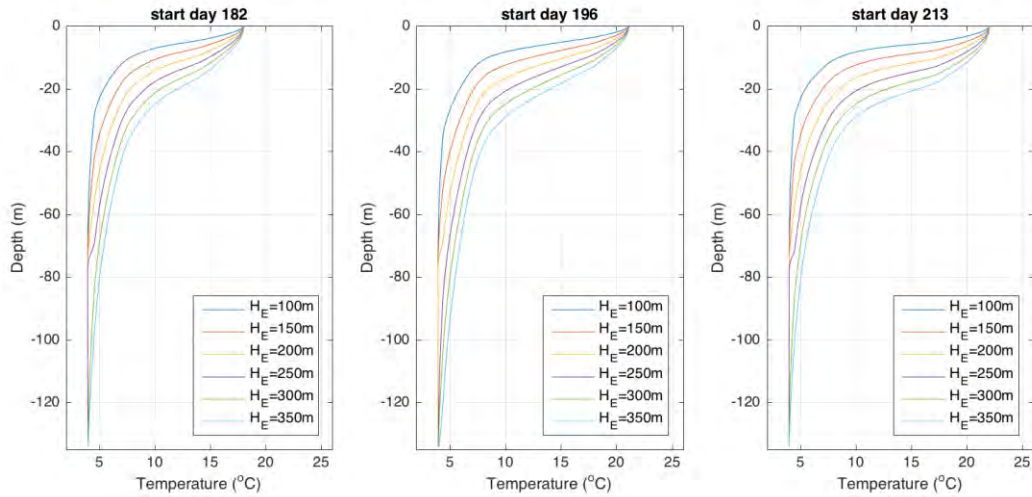


Figure 20. Additional initial conditions used to test sensitivity to epilimnion depth for three start dates.

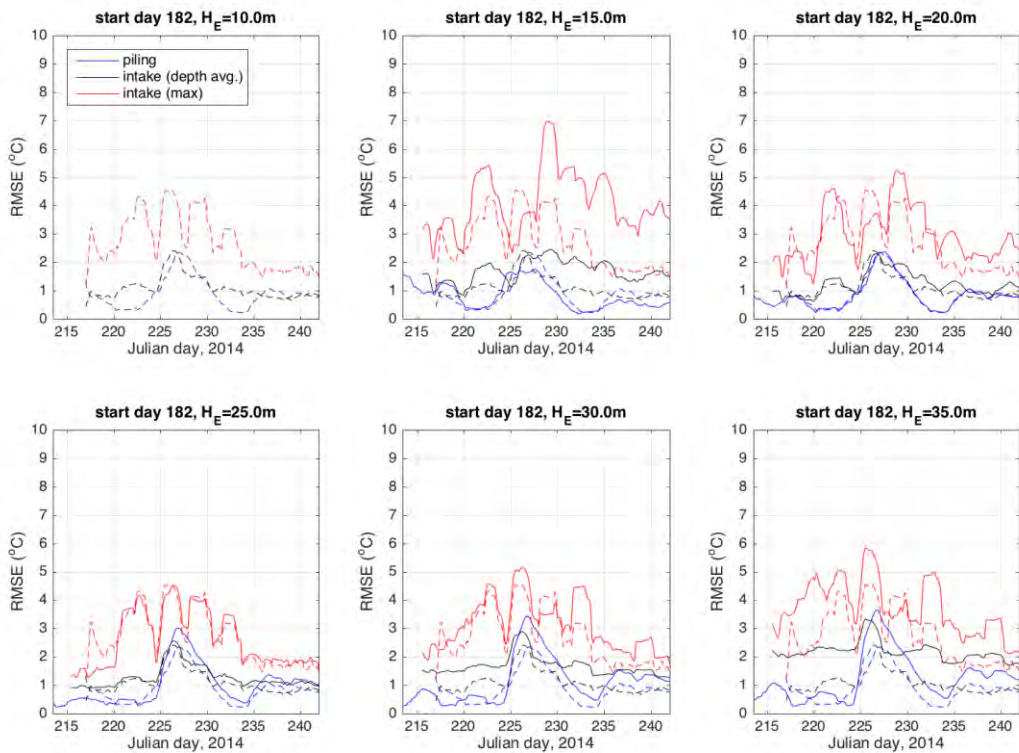


Figure 21. Further test of sensitivity to initial epilimnion depth. Root mean square error (RMSE) is a 2-day running average, comparing field data to simulation. Results for reference simulation are plotted as a dashed line in each window for comparison. RMSE for piling cluster is in blue, depth-averaged RMSE for intake thermistor string is in black, and maximum RMSE for intake thermistor string is in red. No high resolution runs were conducted – all results are for low resolution runs. The reference simulation was initialized with real temperature data on day 217. The rest of the simulations were initialized using re-scaled

temperature profiles measured 2013, with different values of epilimnion depth ( $H_E$ ). Results for more simulation start dates are plotted in Figure 22 and Figure 23.

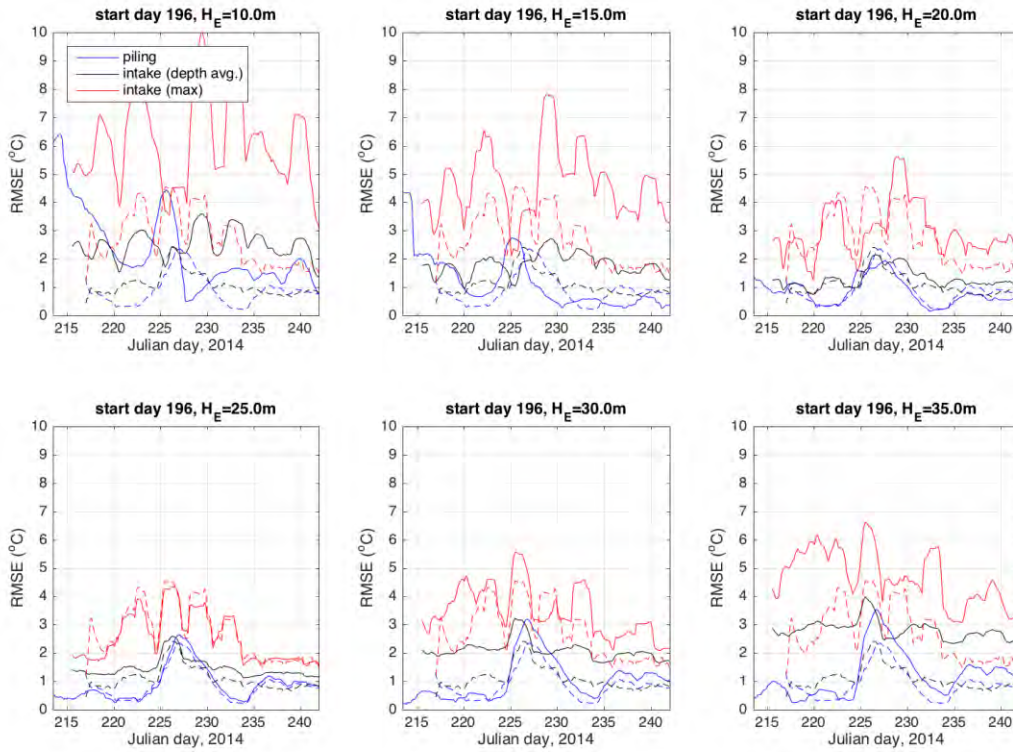


Figure 22. Figure 21, part 2 of 3.

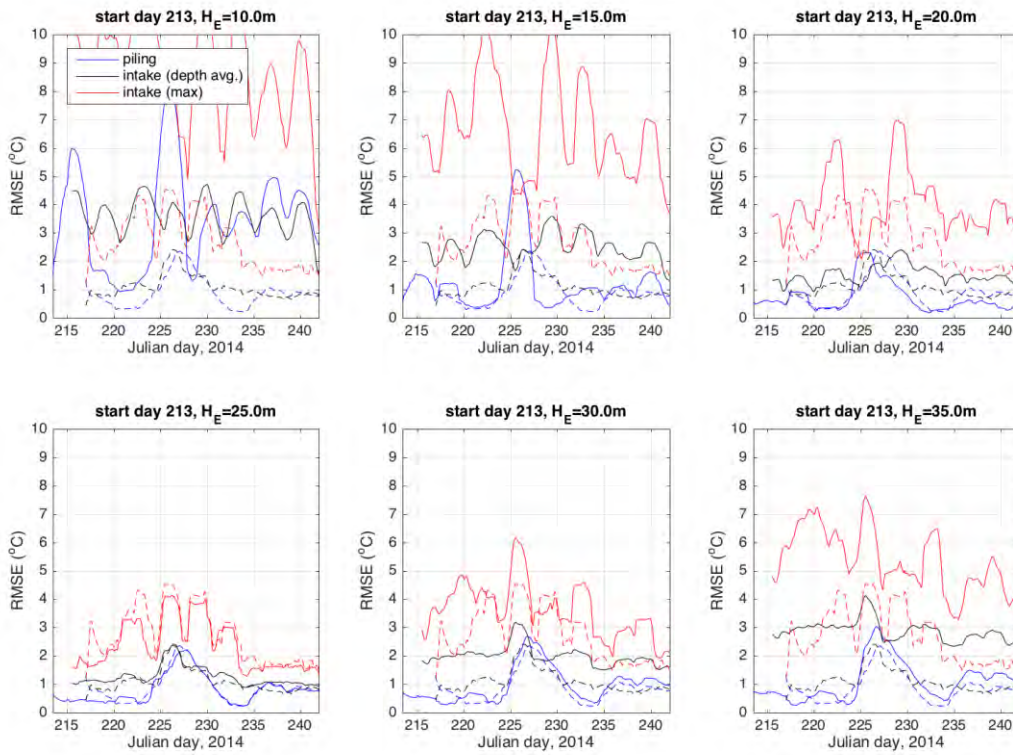


Figure 23. Figure 21, part 3 of 3.

## Bibliography

Lee, Joseph H., and Gerhard H. Jirka. "Multiport diffuser as line source of momentum in shallow water." *Water Resources Research* 16.4 (1980): 695-708.

Wüest, Alfred, and Andreas Lorke. "Small-scale hydrodynamics in lakes." *Annual Review of Fluid Mechanics* 35.1 (2003): 373-412.